

Research Article

Mitochondrial functionality and metabolism in T cells from progressive multiple sclerosis patients

Sara De Biasi¹, Anna Maria Simone², Elena Bianchini³,
Domenico Lo Tartaro⁴, Simone Pecorini⁴, Milena Nasi³,
Simone Patergnani^{5,6}, Gianluca Carnevale³, Lara Gibellini⁴,
Diana Ferraro², Francesca Vitetta², Paolo Pinton^{5,6}, Patrizia Sola²,
Andrea Cossarizza^{4,7} and Marcello Pinti¹ 

¹ Department of Life Sciences, University of Modena and Reggio Emilia, Modena, Italy

² Neurology Unit, Department of Biomedical, Metabolic and Neurosciences, Nuovo Ospedale Civile Sant'Agostino Estense, University of Modena and Reggio Emilia, Modena, Italy

³ Department of Surgery, Medicine, Dentistry and Morphological Sciences, University of Modena and Reggio Emilia, Modena, Italy

⁴ Department of Medical and Surgical Sciences of Children and Adults, University of Modena and Reggio Emilia, Modena, Italy

⁵ Department of Morphology, Surgery and Experimental Medicine, University of Ferrara, Italy

⁶ Maria Cecilia Hospital, GVM Care & Research, E.S. Health Science Foundation, Cotignola, Italy

⁷ Istituto nazionale per le ricerche cardiovascolari, Via Irnerio 48, Bologna, Italy

Patients with primary progressive (PP) and secondary progressive (SP) forms of multiple sclerosis (MS) exhibit a sustained increase in the number of Th1, T cytotoxic type-1 and Th17 cells in peripheral blood, suggesting that the progressive phase is characterized by a permanent peripheral immune activation. As T cell functionality and activation are strictly connected to their metabolic profile, we investigated the mitochondrial functionality and metabolic changes of T cell subpopulations in a cohort of progressive MS patients. T cells from progressive patients were characterized by low proliferation and increase of terminally differentiated/exhausted cells. T cells from PP patients showed lower Oxygen Consumption Rate and Extracellular Acidification Rate, lower mitochondrial mass, membrane potential and respiration than those of SP patients, a downregulation of transcription factors supporting respiration and higher tendency to shift towards glycolysis upon stimulation. Furthermore, PP effector memory T cells were characterized by higher Glucose transporter -1 levels and a higher expression of glycolytic-supporting genes if compared to SP patients. Overall, our data suggest that profound differences exist in the phenotypic and metabolic features of T cells from PP and SP patients, even though the two clinical phenotypes are considered part of the same disease spectrum.

Keywords: flow cytometry · metabolism · mitochondria · multiple sclerosis · T cells



Additional supporting information may be found online in the Supporting Information section at the end of the article.

Correspondence: Prof. Marcello Pinti and Dr. Sara De Biasi
e-mail: marcello.pinti@unimore.it; debiasisara@yahoo.it

Introduction

Multiple sclerosis (MS) is a chronic inflammatory and neurodegenerative disease of the central nervous system (CNS). The pathogenesis of MS is still unknown, but it is generally accepted that the alteration of autoimmune homeostasis plays a major role. The relationship between inflammation and neurodegeneration, and their contribution to the different phases of the disease remains to be fully elucidated [1].

Although CNS inflammation seems to be a key determinant for disease progression and axonal damage in progressive MS, several studies have reported an increased activation of immune cells in peripheral blood from progressive MS patients that could contribute to CNS damage during the progressive phase of the disease and reflect the inflammatory response accumulated in the CNS [2]. Indeed, primary progressive (PP) patients and (SP) secondary progressive patients were shown to exhibit a sustained increase in the number of Th1 and T cytotoxic type 1 cells in peripheral blood, suggesting that the progressive phase of the disease is characterized by a permanent peripheral type 1 immune activation [3]. Differences in naive CD4+ T cell biology identify patients with MS having different rates of development of secondary progression [4]; higher percentages of circulating CD4+ and CD8+ T-bet T cells were found in SP and PP patients, and these values were correlated with the severity of the disease [3]. Moreover, studies have shown that SP patients display low IFN- γ , IL-17 and IL-10 production, while Th17 activation dominates the immunologic milieu of PP patients [5–7]. Overall, there is still no consensus on the prevalence of Th1 and Th17 cells in progressive MS.

Along with their distinct functions, specific T cell lineages also possess unique metabolic profiles that are essential for their function and maintenance and may offer a new direction for a modulation of the immune response [8–10]. Cell activation is accompanied by a switch from a metabolism mainly based upon mitochondrial respiration to a metabolism where the glycolytic flux is prevalent [11]. The regulation of these changes in T cell metabolism is very complex, and far from being clarified [12].

Despite the crucial role of these metabolic changes for the decision of T cell fate after antigen stimulation, there are few data concerning the metabolic profiles of different subsets of T cells from patients with MS. Studies concerning this topic have been carried out mainly on the regulatory T cell (Treg) proliferative potential [13, 14]. Since the factors that determine the fate of Treg activation and metabolic reprogramming are also crucial for the activation of effector and memory cells, it is likely that the impairment observed in Treg cells could be also present in other T cell subsets [15]. In particular, it is not known whether lymphocytes from patients with different forms of MS have different capability to activate pathways that ultimately lead to a switch from respiratory to glycolytic pathways.

For these reasons, we investigated the metabolic changes and mt functionality of T cell subpopulations in a group of untreated progressive MS patients, and sought for differences between the PP and SP disease form. Moreover, we assessed whether there could be differences in the response to the same activating stim-

ulus, whether in progressive patients lymphocytes undergo a differentiation in effector cells instead of memory cells, and which metabolic pathways could lead to this phenomenon.

Results

Differences in T cell differentiation and proliferative capability in PP and SP patients

We first investigated the T cell phenotype of patients and controls by using flow cytometry (gating strategy is shown in Supporting Information Fig. 1A). Among the CD4+ T cell compartment, the percentage of T_{CM} from SP patients is higher than those from CTR (mean \pm SEM, 29.04 ± 2.34 vs 19.88 ± 2.11 , $p = 0.006$) and PP patients displayed higher levels of T_{EM} than SP patients (15.43 ± 2.17 vs 10.89 ± 0.87 , $p = 0.031$) (Fig. 1A). PP patients displayed a lower percentage of CD8+ T_N cells compared to SP patients (25.10 ± 3.98 vs 40.59 ± 3.65 , $p = 0.007$) and CTR (25.10 ± 3.98 vs 38.89 ± 3.92 , $p = 0.021$), and higher levels of CD8+ T_{EMRA} cells if compared to SP patients (54.85 ± 4.95 vs 35.61 ± 3.88 , $p = 0.037$; Fig. 1B). SP, but not PP patients displayed a higher percentage of CD8+ T_{CM} cells compared to CTR (9.31 ± 1.54 vs 4.61 ± 1.10 , $p = 0.022$; Fig. 1B). The expression of PD-1, TIGIT and TIM3, three exhaustion markers, was also analyzed in CD4+ and CD8+ T cells (Supporting Information Fig. 1B), but no differences were found in neither in CD4+ nor in CD8+ T cells (Supporting Information Fig. 1C). Similar levels of activation, evaluated by the expression of HLA-DR and CD38, were found among CD4+ and CD8+ T cells of different groups of progressive patients and CTR (Supporting Information Fig. 1D).

In order to understand if the differences in the immunophenotype between patients and controls were due to a different T cell proliferative capability, we analyzed this function among T subpopulations. Thus, we stimulated T cells with aCD3/aCD28, to mimic T cell activation; as a control, we cultured cells in the presence of IL-7, a homeostatic cytokine that helps T cells in preventing atrophy and apoptosis, and in maintaining resting T cell metabolism [8, 16–18]. CFSE dilution revealed that the total amount of CD4+ and CD8+ T cells were characterized by the same proliferation capability and the same CD69 expression after *in vitro* stimulation (Supporting Information Fig. 1E). Regarding the CD4+ T cell compartment, only T_{EM} cells from PP patients had a percentage of dividing cells lower than CTR (30.70 ± 5.71 vs 56.60 ± 5.73 , $p = 0.009$; Fig. 2A). The other T cell subsets from PP patients displayed the same trend, even if the difference was not statistically significant, likely due to high interindividual variability (Fig. 2A).

Concerning the CD8+ compartment, a similar trend was observed; in the case of T_N cells, lymphocytes from PP patients showed a significant lower proliferation if compared to those from CTR (34.71 ± 4.45 vs 63.90 ± 5.37 , $p = 0.001$) and SP (34.71 ± 4.45 vs 57.30 ± 4.37 , $p = 0.047$; Fig. 2B).

Moreover, cytokine production was measured after *in vitro* stimulation; the gating strategy is shown in Supporting

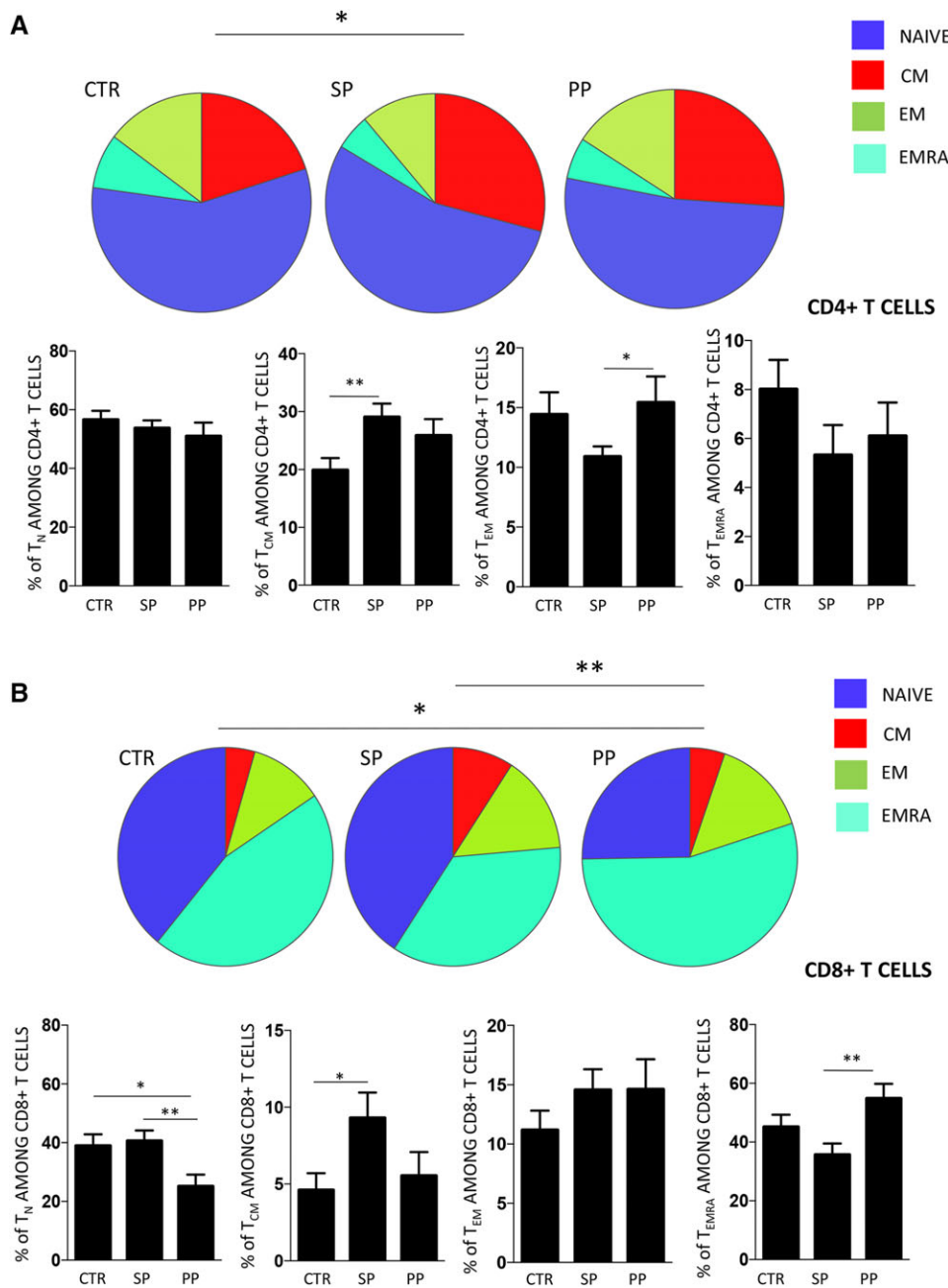


Figure 1. T cell phenotype of progressive patients. Differentiation status of T cells in progressive MS patients. Simplified presentation of incredibly complex evaluations (SPICE) representation of different T cell subsets among CD4+ T cells (A) and CD8+ T cells (B) from SM patients and healthy subjects. Pies compared by permutation test (10,000 permutations). Mann-Whitney t-test * $p < 0.05$, ** $p < 0.01$. Twenty experiments with 1–2 donors per group; $N = 20$ for CTR, 29 for SP, 21 for PP. Data are represented as mean+SEM.

Information Fig. 1F. Similar levels of cytokine producing cells were found among CD4+ T cells, while PP patients, but not SP patients, displayed higher levels of CD8+ T cells producing IFN- γ and IL-17 if compared to CTR (Fig. 3A and B).

Distinct metabolic profiles of T cells from PP and SP patients

As failure to engage the specific metabolic programs impairs the function and differentiation of T cells, we wondered if phenotypic differences of T cells could be explained by differences in their metabolic features. We focused our attention on the CD4+ T cell

subset, which is the principal subset triggering inflammation in MS. We sorted CD4+ T_N and T_{EM} by using the strategy reported in Supporting Information Fig. 1G, and therefore determined their metabolic activity in resting condition and after in vitro stimulation.

In absence of in vitro activation, and in agreement with their quiescent nature, T_N and T_{EM} cells subsets from patients and CTR displayed a low level of metabolic activity. Basal OCR, an indicator of oxidative phosphorylation (OXPHOS), was higher in unstimulated T_N from SP patients if compared to PP patients. After stimulation, basal respiration increased in T_N cells from CTR, SP and PP. Maximal respiration rate and ATP-linked respiration were higher in T_N cells from SP patients than in those from PP

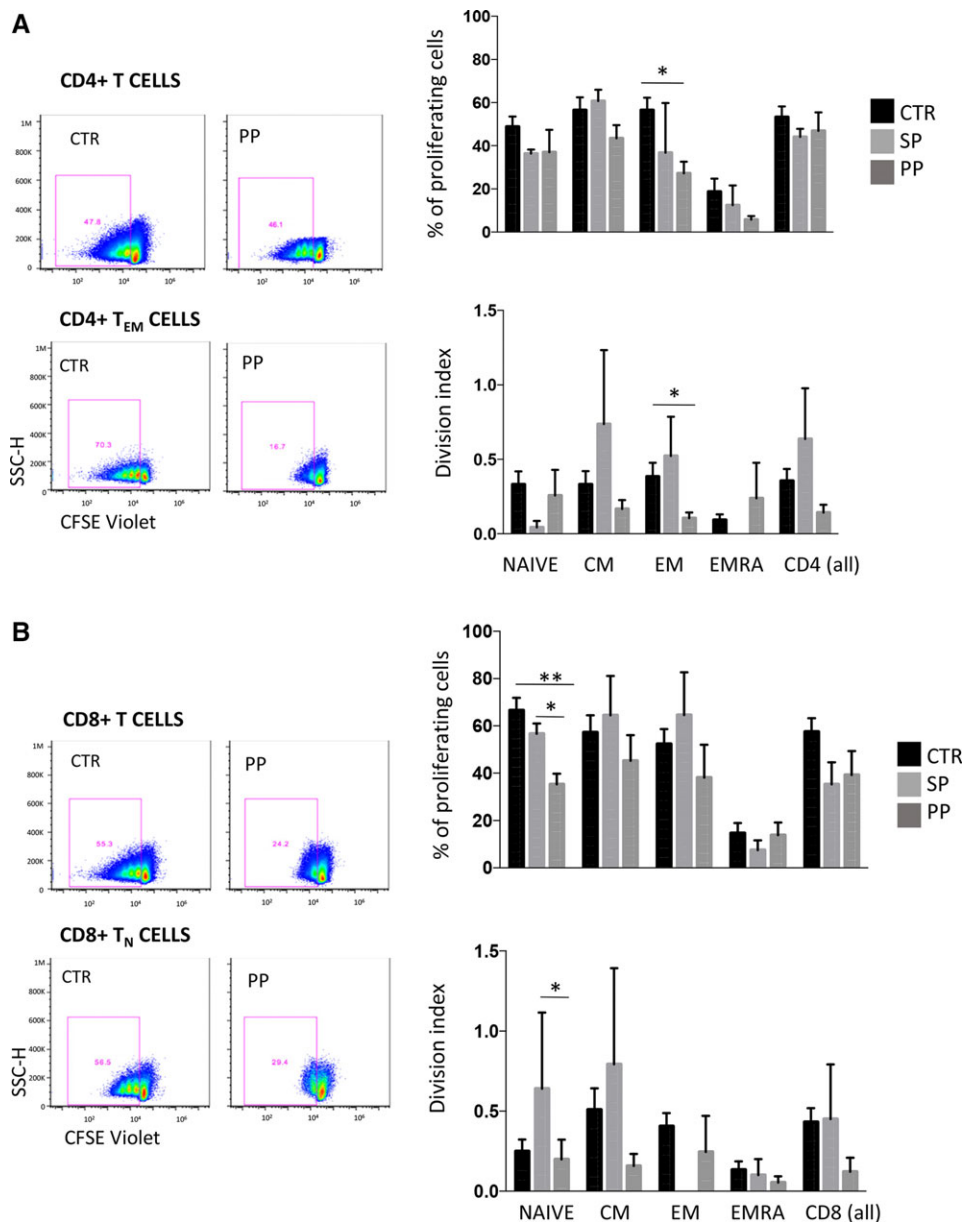


Figure 2. Proliferation of T cells from progressive MS patients and healthy subjects. **A**) Representative dot plot of proliferation tests (evaluated by CFSE dilution) of different subpopulations of CD4+ T cells coming from SP, PP and CTR (upper panel) after 6 days of stimulation with anti-CD3/CD28. Histograms show the percentage of proliferating cells and proliferation index of CTR, SP and PP patients. Mann-Whitney and Wilcoxon t-test $*p > 0.05$, $**p < 0.01$. Three experiments with 1–4 donors per group; $N = 12$ for CTR, 3 for SP, 6 for PP. Data are represented as mean \pm SEM. **(B)** Representative dot plot of proliferation tests (evaluated by CFSE dilution) of different subpopulations of CD8+ T cells coming from SP, PP and CTR (upper panel) after 6 days of stimulation with anti-CD3/CD28. Histograms show the percentage of proliferating cells and proliferation index of CTR, SP and PP patients. Mann-Whitney and Wilcoxon t-test $*p > 0.05$, $**p < 0.01$. Three experiments with 1–4 donors per group; $N = 12$ for CTR, 3 for SP, 6 for PP. Data are represented as mean \pm SEM.

patients. A similar trend could be observed in CD4+ T_{EM} cells, although the differences did not reach significance because of the inter-individual variability (Fig. 4A, B and C). We also estimated ECAR, an indicator of glycolysis on the same cells. Even if we are well aware that the best way for evaluating glycolysis is performing ECAR before and after glucose addition to the medium, we estimated it indirectly by using Mitostress data because of the few numbers of sorted cells available. Basal and maximal ECAR was lower in CD4+ T_N than T_{EM} in CTR and MS patients; moreover, basal ECAR of PP patients was lower than those of SP. This difference was still maintained after in vitro stimulation (Fig. 5A and B). To this regard, we found that both T_N and T_{EM} cells from PP patients had a lower basal and maximal metabolism (OCR and ECAR; Fig. 6A and B, left panels), but a higher capability to upregulate their metabolic activity and, in particular, to increase ECAR, after in vitro stimulation if compared to SP patients. The

OCR/ECAR ratio is similar in all conditions in patients and controls in T_N cells, in agreement with their quiescent status (not shown). Conversely, in T_{EM} cells we observed a clear reduction of the OCR/ECAR ratio in stimulated cells from PP patients, indicating that their T_{EM} cells have a higher tendency to shift from respiration to glycolysis, when required (Fig. 6A and B, right panels).

Mitochondria are smaller and disarranged in T cells from PP patients

As OXPHOS takes place in mitochondria, which play a crucial role in determining the differentiation of T cells into memory or effector cells, we characterized the mt morphology and functionality of T cells from patients and controls. Mitochondrial membrane potential (MMP) was evaluated in CD4+ and CD8+ T_N, T_{CM},

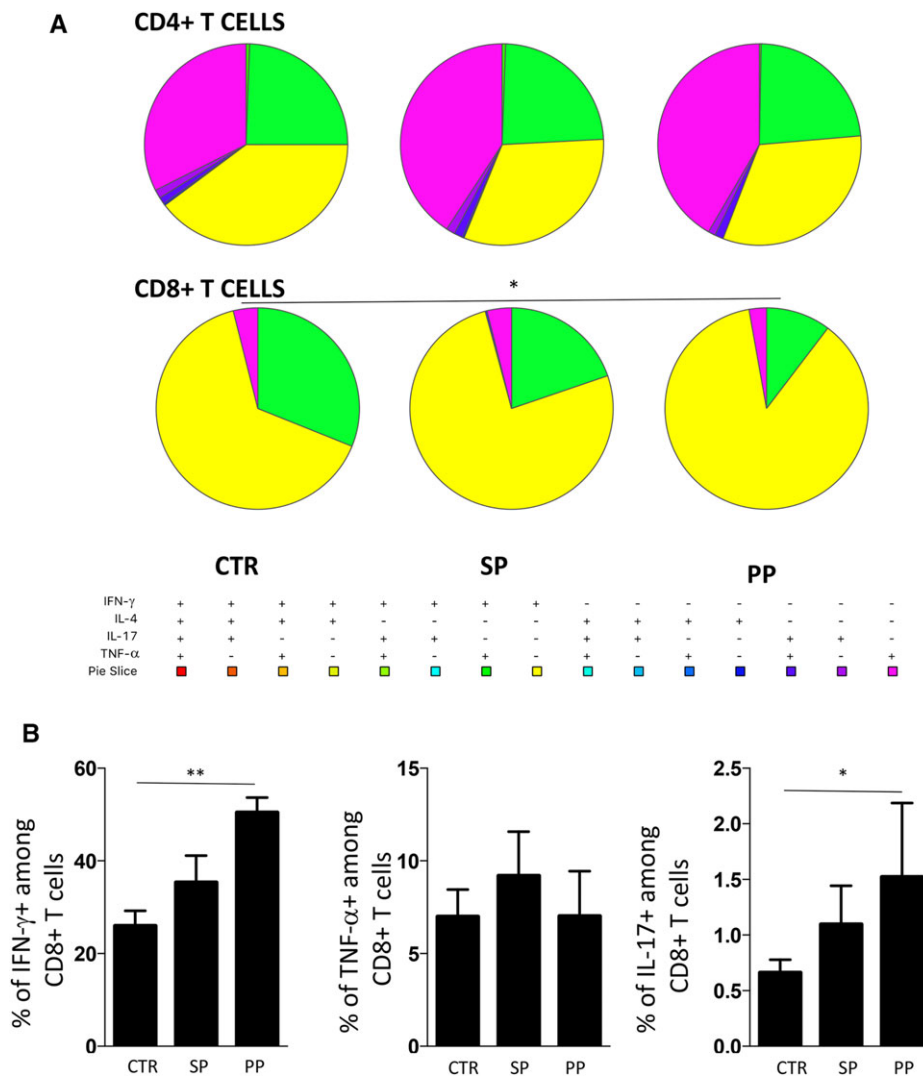


Figure 3. Cytokine production of CD8+ T cells from progressive patients. (A) Simplified Presentation of Incredibly Complex Evaluations (SPICE) representation of T cell producing TNF- α , IFN- γ , IL-17, IL-4. Pies compared by permutation test (10 000 permutations). Mann-Whitney t-test * $p < 0.05$, ** $p < 0.001$. Twenty experiments with 1–2 donors per group; N = 20 for CTR, 29 for SP, 21 for PP. Data are represented as mean+SEM. (B) Percentage of CD8+ T cells producing IFN- γ , TNF- α and IL-17. Mann-Whitney t-test * $p < 0.05$, ** $p < 0.01$. Twenty experiments with 1–2 donors per group; N = 20 for CTR, 29 for SP, 21 for PP. Data are represented as mean+SEM.

T_{EM} , T_{EMRA} before and after in vitro stimulation (data regarding CD8+ T cells are reported in Supporting Information Fig. 2A). MMP decreased in all CD4+ T cells subpopulations after in vitro stimulation, but the decrease was more evident in T_{CM} from SP ($p = 0.039$) and PP patients ($p = 0.022$) than from controls. Concerning T_N cells, PP patients displayed a more marked decrease in MMP compared to those from SP patients ($p = 0.019$) and CTR ($p = 0.003$). No differences were found in all other T cell subsets (Fig. 7A).

Mitochondrial superoxide represents a crucial second messenger for TCR signaling [19]. For this reason, we analyzed its levels in different subpopulations of T cells before and after 30' of in vitro stimulation, by using MitoSox Red (Supporting Information Fig. 2B). The overall level of ROS production remained low even after brief in vitro stimulation. Moreover, no differences were found among different groups of patients and CTR, ruling out the possibility that mtROS could play a role in determining the differences observed in T cell activation and differentiation.

Moreover, we analyzed mt mass in CD4+ T_N , T_{CM} , T_{EM} , T_{EMRA} before and after in vitro stimulation (Fig. 7B). CD4+ T_N cells

were characterized by a lower mt mass than CD4+ T_{EM} cells from CTR ($p = 0.014$), SP ($p = 0.026$) and PP ($p = 0.061$) patients. After in vitro stimulation, we observed small, but significant, changes in the mt mass, with CD4+ T cell subpopulations being most affected. Primary and secondary progressive patients displayed a distinct profile: PP patients' mt mass was lower than that found in SP patients in T_N ($p = 0.030$), T_{CM} ($p = 0.015$), T_{EM} ($p = 0.035$) and T_{EMRA} ($p = 0.049$). Finally, PP but not SP patients displayed a tendency -though not significant- to a lower mt mass than that found in T_{EM} from CTR ($p = 0.079$). Western blotting analysis of TOM20, a mt import receptor subunit used as indicator of mt mass, in sorted CD4+ T_N confirmed flow cytometric data (Fig. 7C), while we obtained contrasting data regarding T_{EM} subset (Fig. 7D). Concerning CD8+ T cells, mt mass in T_N cells was lower than in T_{CM} from CTR ($p = 0.022$), SP ($p = 0.005$) and PP patients ($p = 0.001$; Supporting Information Fig. S2C).

Subsequently, we wondered if differences in MMP were mirrored by a different ultrastructural organization of the organelles. Thus, we looked at mitochondria in sorted CD4+ T_N and T_{EM} cells

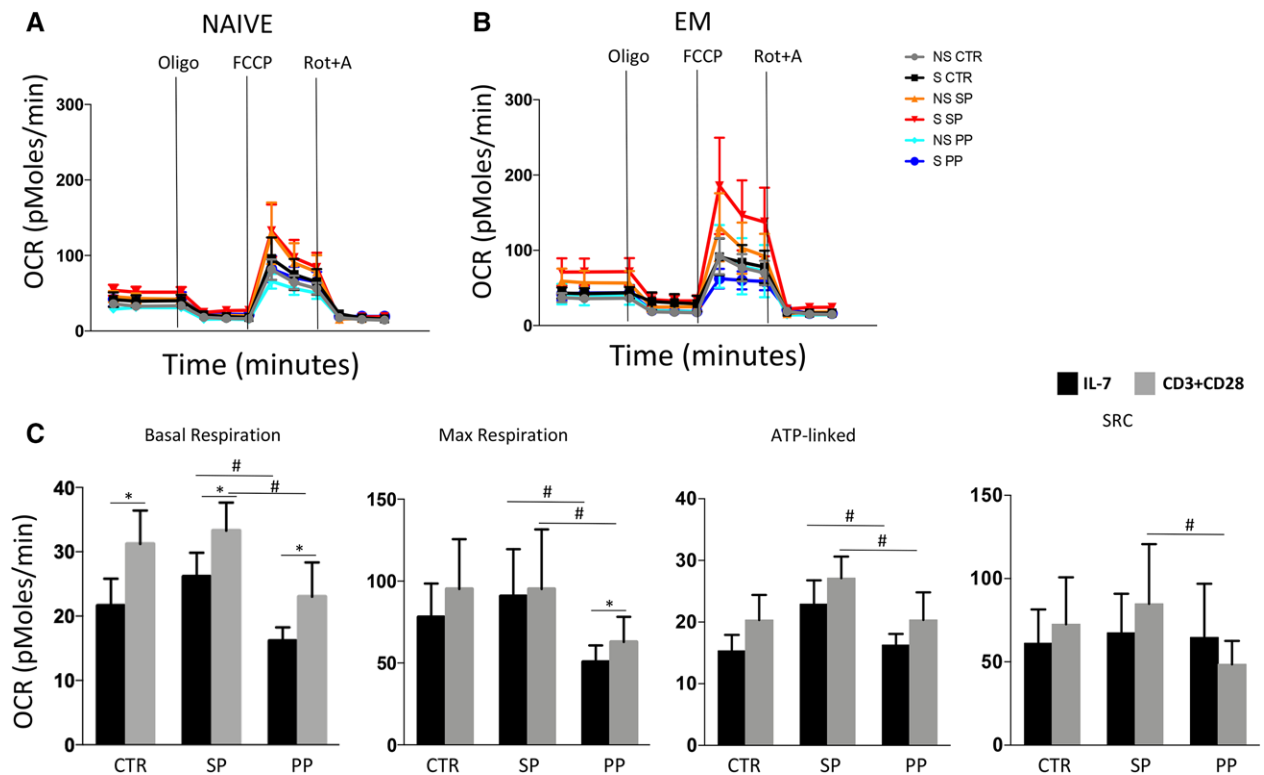


Figure 4. Oxygen consumption rate of T cells from progressive patients. (A) Kinetic profile of OCR in CD4+ T_N cells stimulated with IL-7 or anti-CD3/CD28 for 16 h. OCR was measured in real time, under basal condition and in response to indicated mitochondria inhibitors: oligomycin, FCCP, Antimycin A and Rotenone. After obtaining basal respiration, the cells were subjected to 2 μ M oligomycin, which inhibits ATP synthase and limits mitochondrial OCR. Subsequently, FCCP (cyanide-4-(trifluoromethoxy)phenylhydrazone) was added (1.5 μ M), which uncouples mitochondrial respiration and maximizes OCR, finally Antimycin and Rotenone A, which inhibit mitochondrial respiratory chain, were injected (1 μ M). Ten experiments with 1–2 donors per group, each analysed in triplicate; N = 12 for CTR, 10 for SP, 10 for PP. Data are represented as median \pm SEM. (B) Kinetic profile of OCR in CD4+ T_{EM} cells stimulated with IL-7 or anti-CD3/CD28 for 16 h. OCR was measured in real time, under basal condition and in response to indicated mitochondria inhibitors: oligomycin, FCCP, Antimycin A and Rotenone. After obtaining basal respiration, the cells were subjected to 2 μ M oligomycin, which inhibits ATP synthase and limits mitochondrial OCR. Subsequently, FCCP (cyanide-4-(trifluoromethoxy)phenylhydrazone) was added (1.5 μ M), which uncouples mitochondrial respiration and maximizes OCR, finally Antimycin and Rotenone A, which inhibit mitochondrial respiratory chain, were injected (1 μ M). Indices of mitochondrial respiratory function, calculated from cells OCR profile: basal OCR, Maximal OCR, ATP-linked OCR, spare respiratory capacity. Mann–Whitney and Wilcoxon t-test * p > 0.05, ** p < 0.01. Ten experiments with 1–2 donors per group, each analysed in triplicate; N = 12 for CTR, 10 for SP, 10 for PP. Data are represented as mean \pm SEM. NS = not stimulated (IL-7); S = anti-CD3/CD28 stimulated. (C) Indices of mitochondrial respiratory function calculated from cells OCR profile in CD4+ T_N cells stimulated with IL-7 or anti-CD3/CD28 for 16 h. OCR was measured in real time, under basal condition and in response to indicated mitochondria inhibitors: oligomycin, FCCP, Antimycin A and Rotenone. Basal OCR, Maximal OCR, ATP-linked OCR, spare respiratory capacity. * p < 0.05, ** p < 0.01. Mann–Whitney and Wilcoxon t-test * p > 0.05, ** p < 0.01. Ten experiments with 1–2 donors per group, each analysed in triplicate; N = 12 for CTR, 10 for SP, 10 for PP. Data are represented as mean+SEM.

from CTR, SP and PP patients by electron microscopy. Representative electron micrographs of mitochondria from unstimulated and stimulated T_N and T_{EM} cells are reported in Fig. 8A. Quantitative analysis showed that, after stimulation, mitochondria of CD4+ T_N cells from PP patients had lower values of aspect ratio and form factor if compared to SP and controls, corresponding to objects that are, on average, shorter, more circular, and less branched (Fig. 8B, left panels). Analysis of mitochondrial area – a parameter associated with mt dimensions – and perimeter confirmed that mitochondria from PP patients were smaller and more rounded (Fig. 8B, right panels). When we looked at mitochondria from CD4+ T_{EM} cells, we observed a similar behavior, and quantitative analysis indicates that mitochondria from T_{EM} cells from PP patients were smaller, shorter and more circular than those from SP patients (Fig. 8C).

Glycolysis is increased in progressive patients

Since OXPHOS and mitochondria resulted different in T cells from PP and SP patients, we analyzed the expression of genes involved in the maintenance of OXPHOS or in the activation of glycolysis after TCR engagement in isolated T_N and T_{EM} cells. We analysed a set of seven genes (c-Myc, HIF-1 α , ERR α , BCL-6, FOXO1, KLF2 and MST1) that act as key metabolic regulators.

Concerning glycolysis activating genes, an up-regulation of c-Myc was observed only in CD4+ T_N cells from CTR and, to a lesser extent, in SP patients, while T_N cells from PP patients did not show any significant increases (Fig. 9A, left panel). HIF-1 α , which is crucial for glycolysis uptake and Th17 differentiation, was upregulated in CD4+ T_{EM} cells of SP and PP patients compared to unstimulated cells after in vitro stimulation,

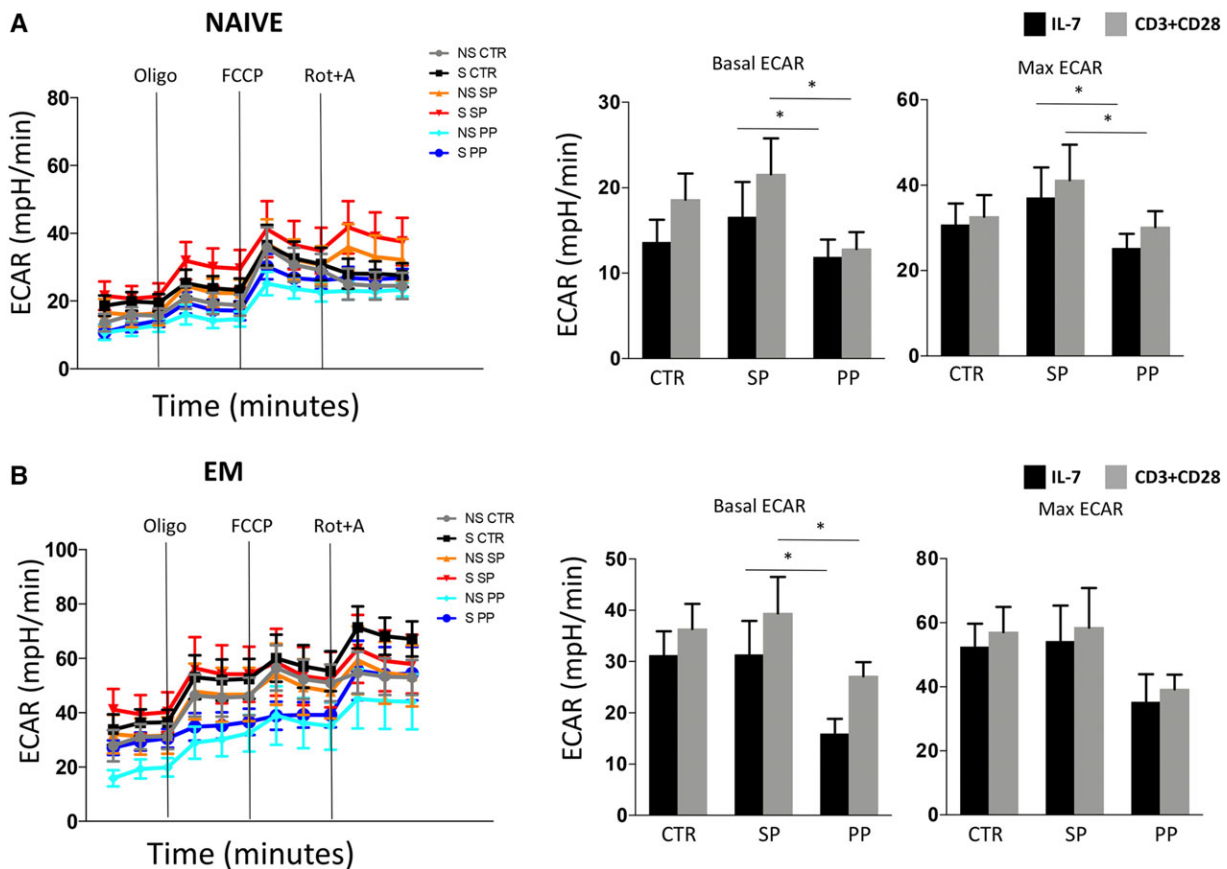


Figure 5. Extracellular acidification rate of T cells from progressive patients. (A) Kinetic profile of ECAR and indices of extracellular acidification rate, calculated from cells ECAR profile in CD4⁺ T_N cells stimulated with IL-7 or anti-CD3/CD28 for 16 h. ECAR was measured in real time, under basal condition and in response to indicated mitochondria inhibitors: oligomycin, FCCP, Antimycin A and Rotenone. Basal ECAR, Maximal ECAR. Mann-Whitney and Wilcoxon t-test. **p* < 0.05, ***p* < 0.01. Ten experiments with 1–2 donors per group, each analysed in triplicate; *N* = 12 for CTR, 10 for SP, 10 for PP. Data are represented as mean ± SEM. (B) Kinetic profile of ECAR and indices of extracellular acidification rate, calculated from cells ECAR profile in CD4⁺ T_{EM} cells stimulated with IL-7 or anti-CD3/CD28 for 16 h. ECAR was measured in real time, under basal condition and in response to indicated mitochondria inhibitors: oligomycin, FCCP, Antimycin A and Rotenone. Basal ECAR, Maximal ECAR. Mann-Whitney and Wilcoxon t-test. **p* < 0.05, ***p* < 0.01. Ten experiments with 1–2 donors per group, each analysed in triplicate; *N* = 12 for CTR, 10 for SP, 10 for PP. Data are represented as mean ± SEM.

and its expression was higher in stimulated cells of SP patients in comparison to those of PP patients (Fig. 9A, central panel).

When we measured the expression of genes which are important for T cell quiescence and OXPHOS maintenance, we observed that in vitro stimulation determined a decrease of FOXO1 in CD4⁺ T_N cells of PP and SP patients, but not in CTR; such a decrease appeared greater in PP patients (Fig. 9A, right panel). No significant differences were observed for the other analysed genes (not shown).

The above results suggest that T cells from PP and SP patients are metabolically different, at least regarding OXPHOS and mt functionality. In agreement with these observations, important differences were noted among T cell subsets in their capability to activate glycolysis in patients and controls.

We first analyzed the activation of mTOR, and of its downstream targets involved in the activation of glycolysis. The expression of mTOR did not show significant differences between

patients and controls, as well as T_N and T_{EM} cells (Fig. 10A and B). After stimulation, we observed a tendency -although not significant - to increase in the ratio between phospho-mTOR (pmTOR) and mTOR, which was more evident in T_{EM} cells, in agreement with their more rapid capability to undergo activation upon stimulation. While no difference was found among groups in T_N cells, in the case of T_{EM} cells, the increase in the phosphorylated form was more evident in controls and PP patients than SP patients. PP patients displayed the lowest levels of AKT and when stimulated, we did not observe any relevant variation in its phosphorylation in any of the groups. Conversely, when we analyzed the phosphorylation of the ribosomal protein S6 (pS6), a downstream pathway of mTOR, after in vitro activation, CD4⁺ T_{EM} cells from PP patients displayed a higher percentage of phosphorylated cells than those coming from CTR (*p* = 0.013) and SP patients (*p* = 0.032; Fig. 9B). As expected, we found the lowest number of pS6-positive cells among T_N subsets in all groups, with a trend to a higher number in SP and PP patients. No differences were found in pS6 levels

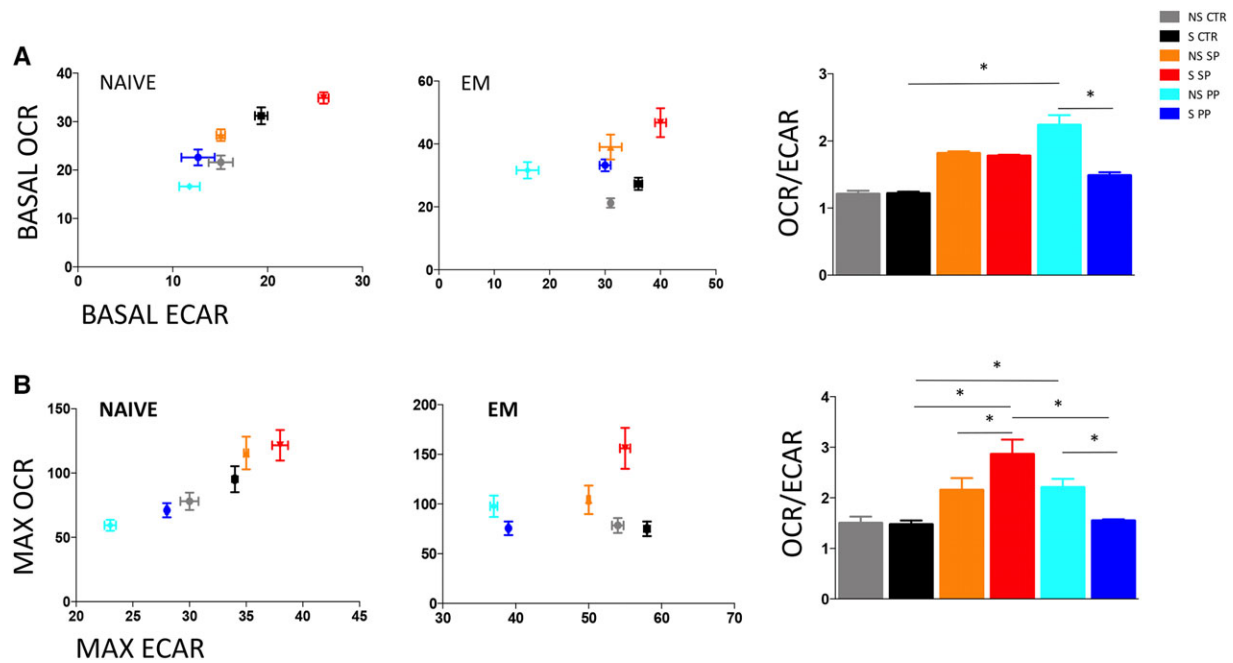


Figure 6. Metabolic profile of T cells from progressive patients. (A) Basal OCR versus basal ECAR in T_N (left panel) and T_{EM} (middle panel) and OCR to ECAR ratio (OCR/ECAR) of T_{EM} cells (right panel) before and after in vitro stimulation. Mann–Whitney and Wilcoxon *t*-test. * $p < 0.05$, ** $p < 0.01$. * $p < 0.05$, ** $p < 0.01$. Ten experiments with 1–2 donor per group, each analysed in triplicate; $N = 12$ for CTR, 10 for SP, 10 for PP. Data are represented as mean \pm SEM. (B) Maximal OCR versus Maximal ECAR in T_N (left panel) and T_{EM} (middle panel) and OCR to ECAR ratio (OCR/ECAR) of T_{EM} cells (right panel) before and after in vitro stimulation. Mann–Whitney and Wilcoxon *t*-test. * $p < 0.05$, ** $p < 0.01$. Ten experiments with 1–2 donor per group, each analysed in triplicate; $N = 12$ for CTR, 10 for SP, 10 for PP. Data are represented as mean \pm SEM.

among different subsets of CD8⁺ T cells (Supporting Information Fig. 3A).

Accordingly, the expression of GLUT1, a receptor crucial for the uptake of glucose needed to foster glycolysis and sustain proliferation, presents important differences in patients and controls. Indeed, we analyzed its expression in CD4⁺ T_N , T_{CM} , T_{EM} , T_{EMRA} before and after in vitro stimulation (Fig. 11A). In resting condition, the expression of GLUT1 was higher in PP patients than SP patients in T_N ($p = 0.038$), T_{EM} ($p = 0.015$) and T_{EMRA} ($p = 0.001$) suggesting that T cells from PP patients are intrinsically more efficient in the up-take of glucose than SP patients. These differences were maintained after in vitro activation of T cells; confocal microscopy analysis showed that activation determines not only an increase in the levels of the protein, but also a redistribution of the receptor from the cytoplasm to the membrane (Fig. 11A, middle panel). A similar level of GLUT1 expression was found among CD8⁺ T cell subsets (Supporting Information Fig. 3B).

Then, we analyzed plasma lactate levels as a parameter that could, at least in part, reflect the presence of metabolic alterations of T cells in progressive patients, and that might have an impact in disease progression. Plasma levels of lactate and pyruvate were measured in both groups of patients and healthy subjects. Both PP and SP patients were characterized by higher levels of lactate than healthy subjects, but SP patients presented higher levels than PP patients. Similar pyruvate concentrations were found among patients and healthy subjects (Fig. 11B).

Finally, in order to relate the above findings on T cells to the clinical disease status, we analyzed the EDSS, which quantifies

disability, and the MSSS, which determines the progression of disability in patients with MS. No correlation was observed among these parameters and phenotypic and functional parameters measured in T cells.

Discussion

MS is considered an autoimmune disease, triggered by autoreactive lymphocytes mounting aberrant responses against CNS autoantigens, whose nature still remains elusive [20]. According to the CNS-extrinsic (peripheral) model, autoreactive CD4⁺ T cells are activated in the periphery and infiltrate the CNS, leading to inflammation and tissue damage [21]. Essential aspects for T cell fate and function are cellular metabolism and its dynamic reprogramming in response to its different needs. However, only very few studies have analyzed metabolic profiles and mt functionality of T cells in MS patients. Thus, it remains unclear if changes occur in T lymphocyte of MS patients and how they could impact on the natural course of the disease.

In this study, for the first time, we performed a comprehensive characterization of the phenotypic, functional and metabolic features of T cells from a total of 53 patients with primary or secondary progressive forms of MS. Importantly, being aware that T lymphocytes in a different state of activation and differentiation rely on distinct metabolic programs for their functioning [22], we analyzed metabolic parameters in different T cell subsets before and after in vitro stimulation. Our investigation focused on the

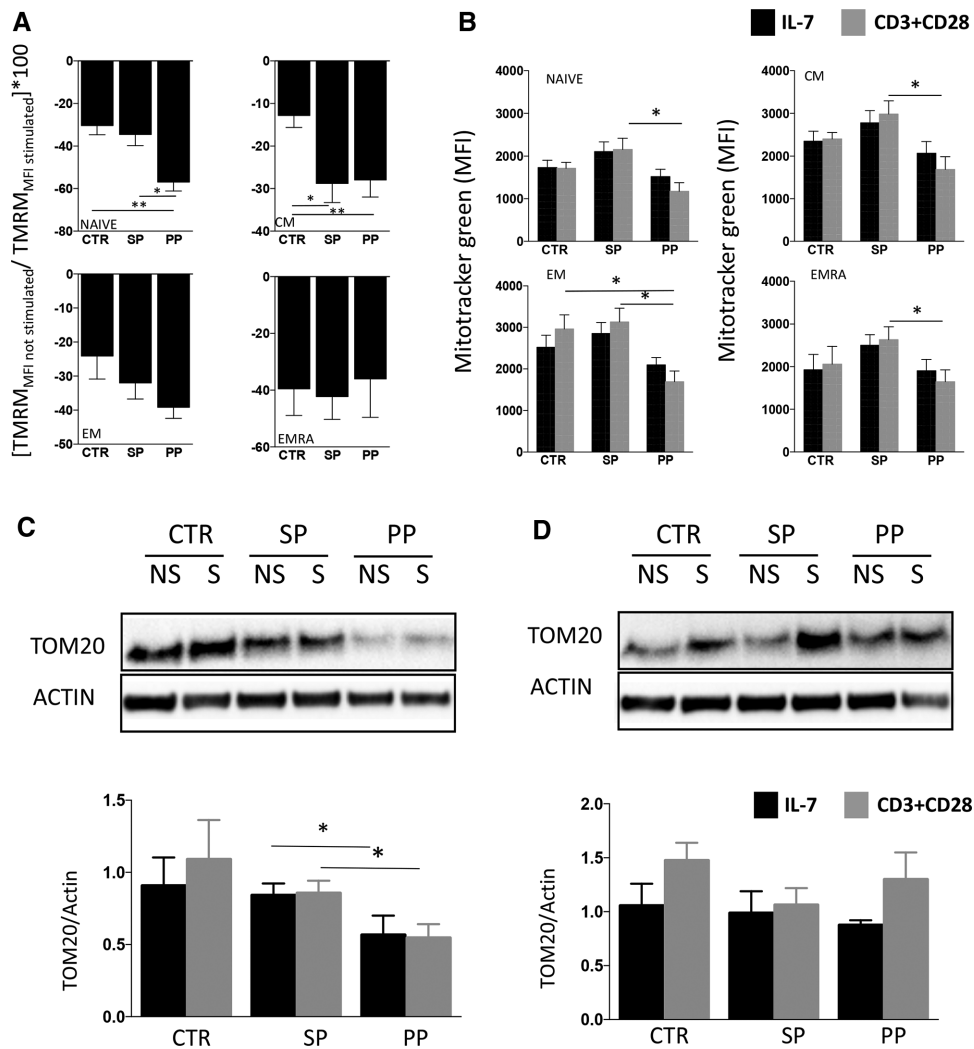


Figure 7. Mitochondrial phenotype and functionality. (A) Analysis of mitochondrial membrane potential of CD4⁺ T cell subsets by staining with TMRM. MMP quantification in cells sorted from fresh blood from CTR, SP and PP. Black bars represent unstimulated cells, while grey bars represent stimulated cells. Mann–Whitney and Wilcoxon t-test. **p* < 0.05, ***p* < 0.01. Eight experiments with 1–3 donors per group; *N* = 8 for CTR, 13 for SP, 11 for PP. Data are expressed as $\text{TMRM}_{\text{MFI not stimulated}} / \text{TMRM}_{\text{MFI stimulated}} * 100$, and represented as mean ± SEM. (B) Analysis of mitochondrial mass of CD4⁺ T cell subsets by staining with Mitotracker green. Mitotracker green MFI quantification in cells sorted from fresh blood from CTR, SP and PP. Black bars represent unstimulated cells, while grey bars represent stimulated cells. Mann–Whitney and Wilcoxon t-test. **p* < 0.05, ***p* < 0.001. Eight experiments with 1–3 donors per group. CTR = 8, SP = 13, PP = 11, data are represented as mean ± SEM. (C) Immunoblot of TOM20 and ACTIN in human freshly isolated CD4⁺ T_N cells. Black bars represent unstimulated cells, while grey bars represent stimulated cells. One representative example of two independent experiments is shown. Graphs show the relative densitometric quantitation of the gels shown. Mann–Whitney and Wilcoxon t-test. **p* < 0.05, ***p* < 0.001. One experiment with 3 samples per group. Data are represented as mean ± SEM. (D) Immunoblot of TOM20 and ACTIN in human freshly isolated CD4⁺ T_{EM} cells. Black bars represent unstimulated cells (IL-7), while grey bars represent stimulated cells (anti-CD3/CD28). One representative example of two independent experiments is shown. Graphs show the relative densitometric quantitation of the gels shown. Mann–Whitney and Wilcoxon t-test. **p* < 0.05, ***p* < 0.001. One experiment with 3 samples per group. Data are represented as mean ± SEM.

metabolic features of CD4⁺ T cell subset. To date, studies concerning T cell metabolism in MS have been carried out only on Treg cell proliferative potential [13], or on a heterogeneous T cell population, i.e. CD4⁺ T cells as a whole, giving unreliable results, which do not allow to understand if the differences observed are due to an intrinsic alteration of T cell activation pathways, or to a difference in the relative distribution of CD4⁺ T cell subsets between MS patients and CTR [23].

Our data showed that profound differences exist in the phenotypic and metabolic features of T cells from PP and SP patients,

even though the two clinical phenotypes are considered part of the same disease spectrum, and clinical, imaging, and pathological differences between PP and SP MS are more relative than absolute [24]. This observation is corroborated by several lines of evidence.

Firstly, from a phenotypic point of view, PP patients displayed lower levels of T_N cells along with a higher percentage of T_{EMRA} cells compared to SP patients and CTR. The T_{EMRA} cell subset is a terminally differentiated population, whose frequency in peripheral blood is normally quite low among CD4⁺ T cells [25]. Aging

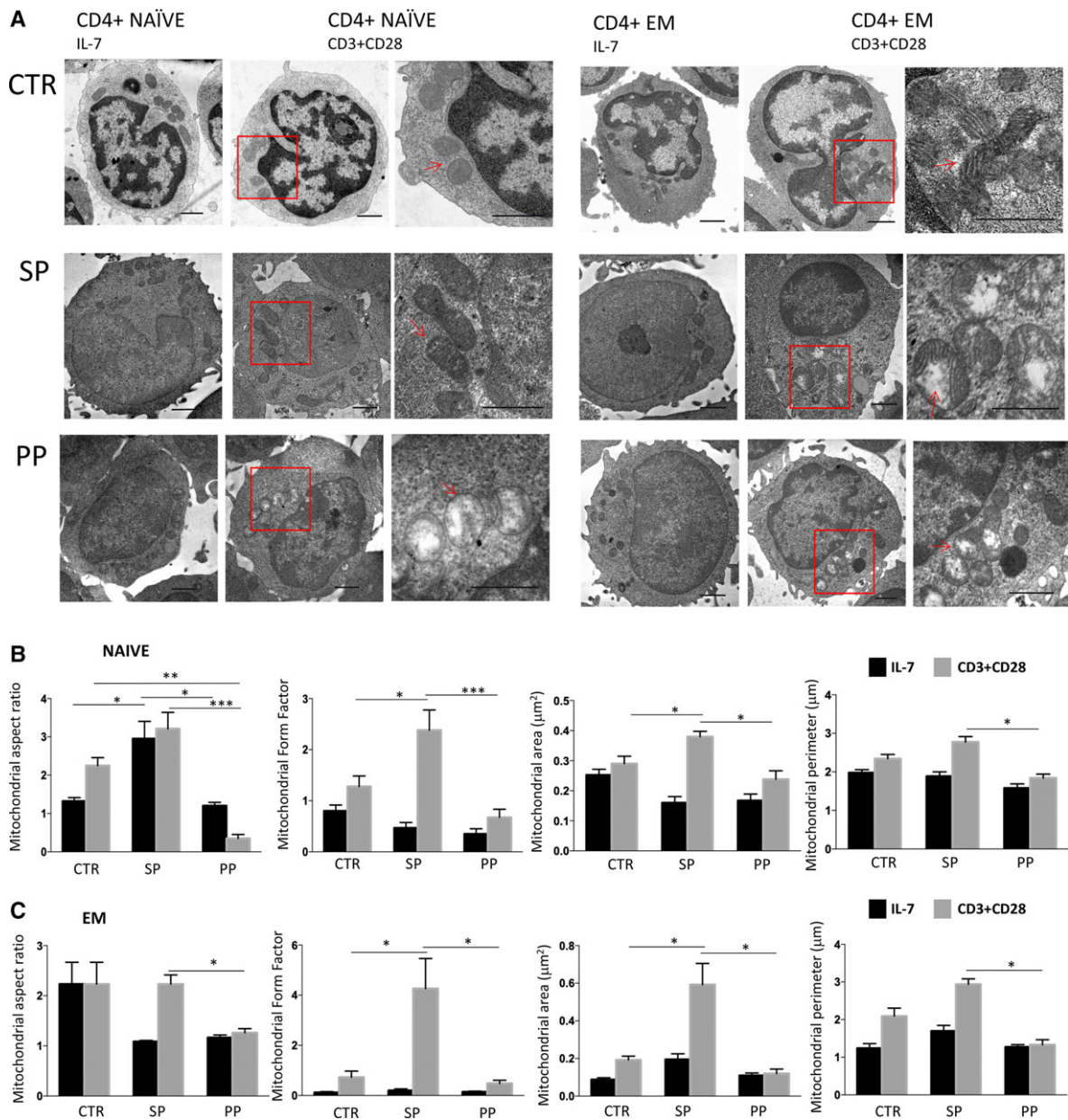


Figure 8. Ultrastructural analysis of mitochondria of T cells from progressive patients. (A) Representative micrographs of sorted T_N and T_{EM} from CTR, SP and PP patients in not stimulated (IL7) and stimulated (CD3/CD28) conditions. An enlarged view of mitochondria from stimulated cells is shown in the third column for each group of subjects. Red arrows indicate mitochondria described in the text. Magnification X50,000 (X80,000 for mitochondria details) Scale bar = 0.5 μm . (B) Morphological analysis of mitochondria in human freshly isolated $CD4^+$ T_N cells. Quantification of ultrastructural mitochondrial alterations and size. Mitochondrial aspect ratio (major axis/minor axis) and form factor (perimeter $^2/4\pi \times$ area), perimeter (μm) and area (μm^2). Black bars represent unstimulated cells (IL-7), while grey bars represent stimulated cells (anti-CD3/CD28). Mann-Whitney and Wilcoxon t-test. * $p < 0.05$, ** $p < 0.01$, *** $p < 0.001$. One experiment with 3 samples per group. Data represented as mean \pm SEM. (C) Morphological analysis of mitochondria in human freshly isolated $CD4^+$ T_{EM} cells. Quantification of ultrastructural mitochondrial alterations and size. Mitochondrial aspect ratio (major axis/minor axis) and form factor (perimeter $^2/4\pi \times$ area), perimeter (μm) and area (μm^2). Black bars represent unstimulated cells (IL-7), while grey bars represent stimulated cells (anti-CD3/CD28). Mann-Whitney and Wilcoxon t-test. * $p < 0.05$, ** $p < 0.01$, *** $p < 0.001$. One experiment with 3 samples per group. Data are represented as mean \pm SEM.

of the immune system is responsible for an increase in the percentage of T_{EMRA} cells due to thymic involution and to persistence of repeated exposure to self or non-self-antigens which causes chronic immune activation and inflammation [26]. This subset abundance along with the low proliferative potential of T_N cells could reflect a chronic and intense inflammation in pro-

gressive patients, which determines persistent adaptive immune system activation, and skewing of T cells towards a more differentiated phenotype, independently from the aging of immune system. Hence, higher levels of this subset in patients affected by the PP form suggest an intense and prolonged T cell stimulation, which probably leads to chronic tissue inflammation. In contrast

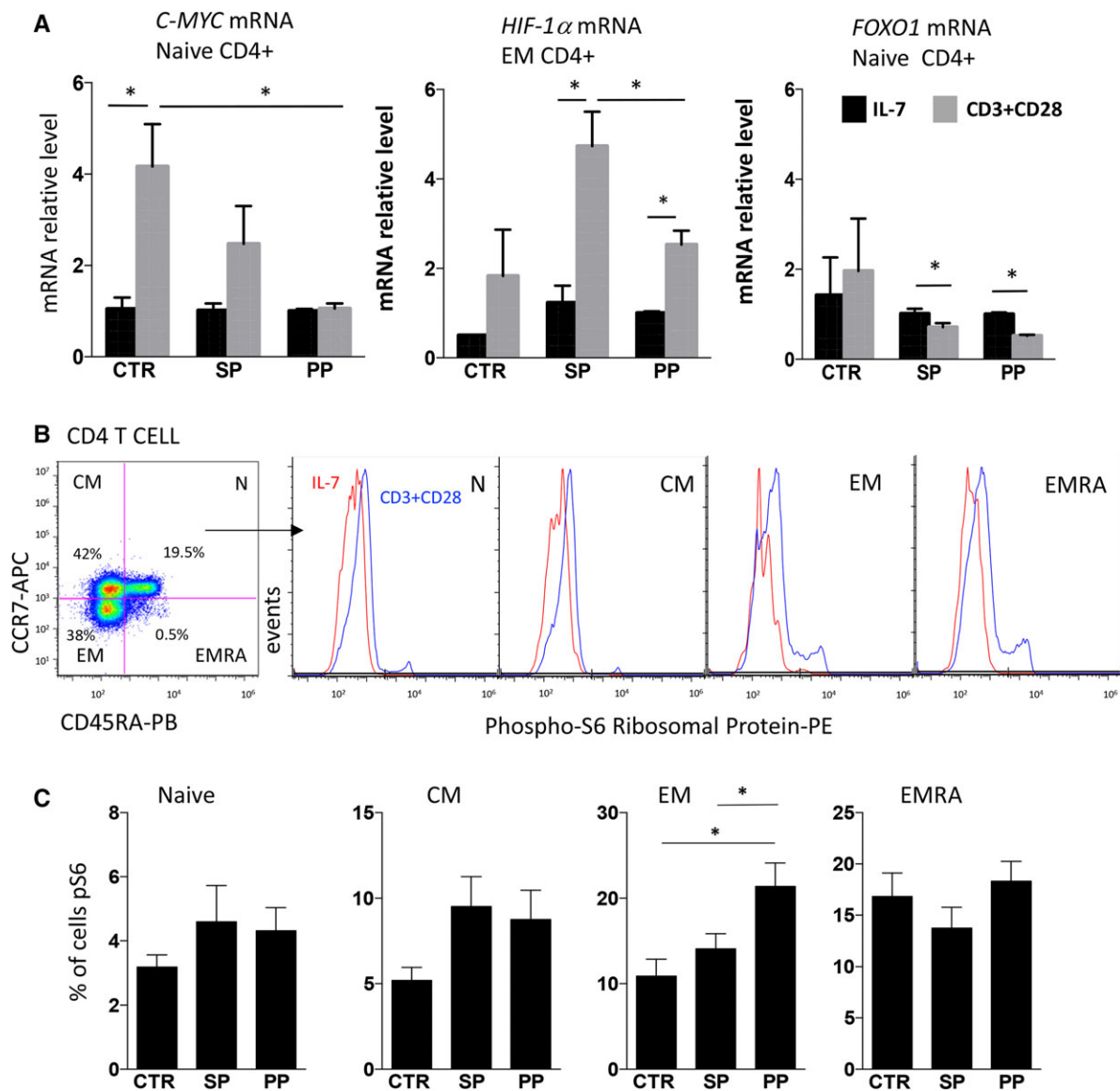


Figure 9. Analysis of glycolytic pathway. (A) Expression analysis of *c-Myc*, *HIF-1α*, *FOXO1* in CD4+ T_N and T_{EM} cells. mRNA level normalized to levels of TATA Binding Protein (TBP) of: *c-Myc* T_N cells, *HIF-1α* in CD4+ T_{EM} cells, *FOXO1* in CD4+ T_N cells. Black bars represent unstimulated cells, while grey bars represent stimulated cells. Mann-Whitney and Wilcoxon *t*-test. **p* < 0.05, ***p* < 0.01. One experiment with 5 samples per group. Data represented as mean ± SEM (B) P-S6 expression in CD4+ T cell subpopulations. Black bars represent unstimulated cells, while grey bars represent stimulated cells. Mann-Whitney and Wilcoxon *t*-test **p* < 0.05, ***p* < 0.01. CTR = 8, SP = 13, PP = 11. Data are expressed as percentage of positive cells and represented as mean ± SEM.

to our results, a decreased frequency of CD8+ T_{EM} and T_{EMRA} T cells in all clinical forms of MS was reported [27]. Such divergence in findings may reflect the various panels of mAbs used and the different surface markers chosen for the flow cytometric analysis, as well as different characteristics in the cohort of progressive patients analyzed (our cohort of progressive patients has a longer disease duration). From a functional point of view PP patients displayed higher level of CD8+ T cells producing IFN- γ and IL-17 if compared to control, confirming data regarding a skewed Th1 and Th17 phenotype in PP patients.

Secondly, mitochondria of T cells from PP and SP patients showed clear differences in terms of mass, shape, average dimen-

sion and membrane potential. Mitochondrial activation has been reported to be critical for T cell proliferation and memory formation by studies *in vitro* as well as *in vivo* [28]. Mitochondria contain all the machinery responsible for cell respiration and a greater mt mass is associated to a rapid recall ability, more OXPHOS and cell longevity, such as the case of memory T cells. Thus, the difference we observed in the T cell phenotype between PP and SP patients can be due, at least in part, to differences in mitochondria that, in turn, determine an easier activation and differentiation of T_N cells to the same stimulus.

T cell receptor signaling induces Ca₂⁺ release, which, in turn, promotes mt activities and ROS generation. mtROS are generated

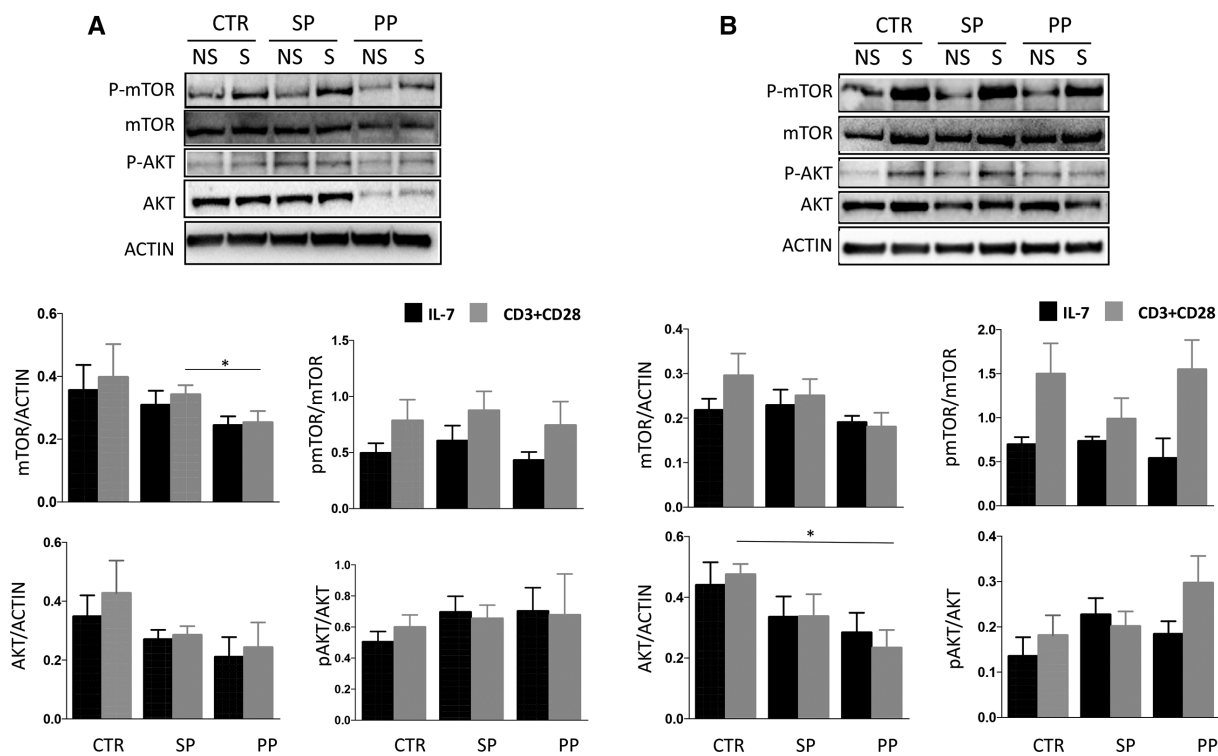


Figure 10. Regulation of mTOR and AKT phosphorylation. (A) Immunoblot for P-mTOR, mTOR, P-AKT, AKT and ACTIN in human freshly isolated CD4⁺ T_N cells. Black bars represent unstimulated cells, while grey bars represent stimulated cells. Graphs show the relative densitometric quantitation of the gels shown. Mann-Whitney and Wilcoxon t-test. **p* < 0.05, ***p* < 0.01. One experiment with 3 samples per group. Data are represented as mean ± SEM. (B) Immunoblot for P-mTOR, mTOR, P-AKT, AKT and ACTIN in human freshly isolated CD4⁺ T_{EM} cells. Black bars represent unstimulated cells, while grey bars represent stimulated cells. Graphs show the relative densitometric quantitation of the gels shown. Mann-Whitney and Wilcoxon t-test. **p* < 0.05, ***p* < 0.01. One experiment with 3 samples per group. Data are represented as mean ± SEM.

rapidly after TCR engagement [29] at complexes I, II, and III of the mt electron transport chain, and superoxide converted from ROS was shown to activate T cells and is considered a messenger during activation [30]. However, we observed similar level of mtO₂⁻ in T_{EM} cells from PP and SP patients, ruling out the possibility that the observed differences in T cell activation and phenotype could be ascribed to a different capability to activate this pathway. Indeed, mtROS appears to be crucial for the synthesis of IL-2 and for the expression of surface markers such as CD69 or CD25 [19]; from this point of view, mtROS levels are in perfect agreement with the observation that CD69 expression is similar in all analysed groups. To this regard, it has been shown that cells with low ROS production are not lacking bioenergetically as they are able to undergo antigen-specific expansion in response to infection and are able to proliferate [31].

As mt fragmentation and dysfunction mark mitochondria for degradation in the selective autophagic process called mitophagy, a role for this process in shaping features of T cells from PP patients could be an intriguing hypothesis. Indeed, once damaged and committed to degradation, mitochondria fragment to sterically allow their selective engulfment in autophagosomes [32]. The difference we observed in mitochondria between PP and SP patients could be due to a differential regulation of mitophagy, which in turn influences the seeding of memory and activation induced cell death of T cells [33]. Accordingly, it could be of interest to inves-

tigate the proteins involved in the multiple mitophagy programs and mt cristae remodeling, along with their ultrastructure in PP and SP patients [34].

Thirdly, gene expression analysis revealed that PP and SP patients were characterized by a different modulation of the molecules orchestrating the metabolic switch and reprogramming. T cell metabolism and its adaptations are dependent upon the coordinate and complex interplay among several signaling pathways and transcription factors [35]. In particular, HIF-1 α is a transcription factor that increases glucose uptake (it binds GLUT1 promoter) when induced by oxidative stress response or mTORC1 [15, 36]. We observed that stimulation increases its expression in T_{EM} cells from PP patients and, to a greater extent, in T_{EM} cells from SP patients. We could speculate that, even if we are detecting gene expression and not the protein, T_{EM} cells from SP patients may be induced earlier to gain a pro-inflammatory profile. In addition to its critical role in the regulation of T cell metabolism, HIF-1 α is a lineage-specific marker of CD4⁺ Th17 cells, which are among the main CD4⁺ T cell subsets implicated in the disease. Increased glycolytic metabolism in Th17 cells also appears to be important in maintaining their Th17 lineage state. Pharmacological inhibition of glucose metabolism by administering 2-deoxyglucose attenuated Th17 cell development and, interestingly, promoted Treg cell development and diminished pathology in a Th17-dependent experimental autoimmune encephalomyelitis

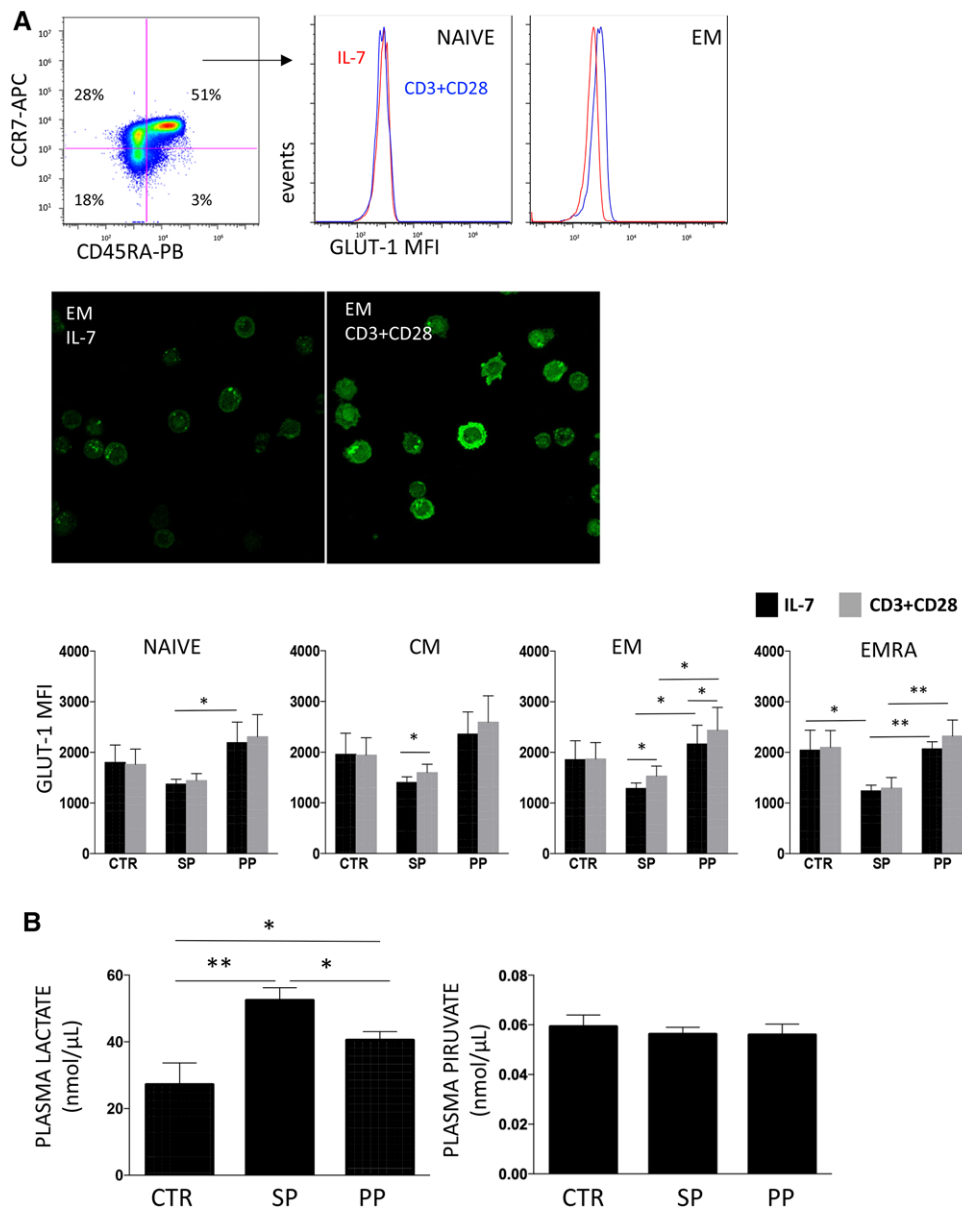


Figure 11. GLUT1 expression in different subpopulations of CD4⁺ T cells. (A) GLUT1 receptor expression in CD4⁺ T cell subpopulations. Representative dot plots, representative confocal image of GLUT1 staining on CD4⁺ T_{EM} cells and histograms of subpopulation of T cells in both not stimulating (IL-7) and stimulating condition (anti-CD3/CD28) after 24 h in CTR, SP and PP. Mann–Whitney and Wilcoxon t-test **p* < 0.05, ***p* < 0.01. CTR = 8, SP = 13, PP = 11, data are expressed as percentage of positive cells and represented as mean \pm SEM. (B) Lactate and pyruvate plasma concentrations as measured by ELISA. Mann–Whitney t-test **p* < 0.05, ***p* < 0.01. Eight experiments with 1–2 donors per group; N = 8 for CTR, 9 for SP, 9 for PP. Data are represented as mean \pm SEM.

model [30]. Indeed, it was reported that lack of HIF-1 α resulted in diminished Th17 development, but enhanced Treg cell differentiation, and protected mice from autoimmune neuroinflammation, suggesting that HIF-1 α -dependent glycolytic pathway orchestrated a metabolic checkpoint for the differentiation of Th17 and Treg cells [37].

Fourthly, the activation of the kinase mTOR, and of its downstream targets involved in the activation of glycolysis appears differently regulated in PP and SP patients. The kinase mTOR is a key metabolic regulator, which induces the expression of GLUT1 [38], and increases protein translation through the phosphorylation of

pS6 by p70S6 kinase upon activation [39]. In addition, it mediates the expression of downstream transcriptional regulators. Even though PP patients upregulate HIF-1 α after stimulation to a lesser extent than SP patients, we found that PP patients were characterized by an upregulation of total GLUT1 in T_{EM} cells (a direct downstream target of the transcription factor). Even if not formally proved by 2-NBDG uptake assay because of the limited number of cells available, the higher level of GLUT1 on the plasma membrane strongly suggests a higher glucose dependency and glucose-mediated energy production. This is in agreement with higher tendency of T_{EM} cells from PP to shift from respiration to glycolysis;

we are well aware that the ideal approach for evaluating glycolysis is performing ECAR before and after glucose addition to the medium. Nevertheless, because of the few number of sorted cells available, we estimated it indirectly by using Mitostress data.

Finally, we found higher levels of plasma lactate in progressive patients than controls, and a higher level in SP than PP patients. Although we are well aware that lactate in plasma can derive from different sources, differences observed in T cell metabolism can account, at least in part, for plasma concentration of glycolytic metabolism. Lactate has been nowadays recognized as an important molecule that bridges metabolism and inflammation [40], and it has been shown that lactate in cerebrospinal fluid and serum is associated with the progression of MS [41]. T cells sense lactate using specific transporters, that inhibit their motility, with a mechanism dependent upon lactate interference with glycolysis. Furthermore, lactate promotes the switch of CD4+ T cells to an IL-17+ subset and reduces the cytotoxic activity of CD8+ T cells [42, 43]. Thus, the higher levels of lactate can also influence the function and response of T cells. Even if we are well aware that we have studied cells in peripheral blood, we cannot exclude that these phenomena could contribute to the formation of ectopic lymphoid structures and autoantibody production in inflammatory sites such as in MS plaques.

The profile we described in this study is reached by patients after more than 20 years of disease duration and, although the progressive phase (regardless of a relapsing-remitting onset) is similar, in clinical terms, in PP and SP patients, the intrinsic difference in T cell metabolism and function we observed suggests that the immunological development of the disease during this long period of time could have been different.

Unregulated and dysfunctional lymphocyte responses are a hallmark of autoimmune and allergic diseases, such as asthma, arthritis, and systemic lupus erythematosus. Similar to exhausted T cells, lymphocytes from patients with these diseases are often repetitively stimulated due to repeated or constant antigen exposure. Because of the unbalanced regulation of these immune responses, T cells from allergic and autoimmune models exhibit an altered metabolic profile compared with healthy lymphocytes. From this point of view, the impairment we observed in the progressive forms of MS, and in particular in the PP form, fits perfectly with the picture depicted in other autoimmune diseases.

Conclusion

Although PP and SP forms present with different disease courses, the inflammatory status and the neurodegenerative process are indistinguishable. In this study, we found similar levels of activation in both groups, but SP and PP patients were characterized by profound differences in the T cell differentiation and proliferative capability, and mitochondria of T_N cells from PP were smaller, depolarized and structurally and functionally compromised. These differences should be taken into account when analyzing the effects of drugs affecting metabolism in progressive patients.

Materials and methods

Patients' selection

Patients were selected at the “Center for Demyelinating Diseases” of the Neurology Unit of Modena (Ospedale Civile S. Agostino Estense - OCSAE, Modena, Italy). Evaluation of entry criteria and subsequent enrollment in the study occurred during patients' planned routine visits. Inclusion criteria were: age ≤ 75 years and diagnosis of MS according to the 2010 revised McDonald Criteria [44]. In particular, we selected untreated PP/SP patients, in order to avoid a potential effect of immunosuppressant drugs on T cell metabolism. As a consequence, enrolled patients had not shown “disease activity” (i.e. relapses, contrast-enhancing lesions on Magnetic Resonance Imaging -MRI- T1-weighted images or new lesions on T2-weighted images) in the previous years (at least two), as they would, otherwise, probably have benefited from immunomodulatory/immunosuppressant treatment.

Patients with concomitant infections (viral or bacterial), steroid treatment in the preceding 30 days and immunomodulatory/immunosuppressive treatment within the previous 6 months were excluded. A total of 53 progressive MS patients were selected:

- 22 MS patients were diagnosed with a PP form;
- 31 MS patients were diagnosed with a SP form.

Twenty six and age-matched healthy subjects (8 males/12 females, mean age \pm SD, 60.8 \pm 4.4), without a history of autoimmune diseases or immunosuppressant/corticosteroid therapy, were chosen as controls (CTR).

The study was carried out in accordance with recommendations of the Prot. n 2483/CE. All subjects gave written informed consent in accordance with the Declaration of Helsinki. The protocol was approved by the Province of Modena Ethical Committee.

The following demographic and clinical variables were collected for all patients at the time of sampling: age, sex, disease duration, Expanded Disability Status Scale (EDSS), Multiple Sclerosis Severity Score (MSSS), presence of “disease progression” (i.e., increasing objectively documented neurologic dysfunction/disability in the preceding year) in the preceding year. The same data was collected during patients' routine follow-up visits (at least every six months) throughout the following two years. Furthermore, at follow-up visits, the presence of “disease progression” was assessed, i.e., an increase in the EDSS score of at least 0.5 points. Mean disease duration was 23.0 \pm 9.0 years and median EDSS at time of sampling was 6.00 (interquartile range -IQR: 6.00-6.50), with no significant differences between PP and SP patients. After a median follow-up period of 2.2 years, median EDSS was still 6.5, but with an IQR of 6.00-7.00 and 26 patients (49%) had shown a progression of at least 0.5 in EDSS scores. Patients who had progressed had a significantly higher EDSS at follow-up (6.94 \pm 0.86 versus 6.00 \pm 1.30; $p = 0.0013$) MSSS was 6.39

Table 1. MS patients' characteristics

	Total	SP	PP
Number of patients	53	31	22
Males, n (%)	17 (32)	10 (32)	7 (32)
Females, n (%)	36 (68)	21 (68)	15 (68)
Age, years ^{a)}	60.7 ± 7.3	60.8 ± 7.3	59.8 ± 7.3
Age at onset, years ^{a)}	38.1 ± 9.7	38.3 ± 9.6	37.5 ± 9.8
Disease duration ^{a)}	22.7 ± 9.4	22.5 ± 9.4	22.6 ± 9.4
EDSS ^{a)}	6.1 ± 1.2	6.1 ± 1.2	6.0 ± 1.2
MSSS ^{a)}	6.1 ± 1.8	6.4 ± 2.2	6.0 ± 1.8

^{a)}Values expressed as mean±SD.

(IQR: 5.16–7.32) at time of sampling and 6.26 (IQR: 5.16–6.66) at follow-up. Table 1 summarizes MS patients' characteristics.

Isolation of peripheral blood mononuclear cells and polychromatic flow cytometry

A maximum of 50 mL of venous blood was collected from each subject into ethylenediaminetetraacetic acid (EDTA) tubes. PMBC were isolated by Ficoll-Hypaque density gradient according to standard procedures and immediately processed.

Immunophenotype of T cells from patients with different forms of MS

A 10-color flow cytometric panel was set up to analyze the percentage of naive (T_N), central memory (T_{CM}), effector memory (T_{EM}), and terminally differentiated (T_{EMRA}) T cells, along with the activation status of T cells. The following mAbs, directly conjugated with different fluorochromes, were used: anti-CD3 PE-Cy5.5, -CD4 AF700, -CD8 APC-Cy7, -CCR7 BV421, -CD45RA PE, -CD38 BV605, -HLA-DR FITC, -CD57 APC, CD28 PE-Cy7 (all from BioLegend, San Diego, CA, USA) along with a marker for cell viability (LIVE/DEAD AQUA, Life Technologies, Eugene, OR, USA). Another panel was set up to analyze the expression of co-inhibitory markers, such as PD-1 (CD279), TIM3 (CD366), TIGIT (CD226) by using anti-PD1 mAbs conjugated with BV421, -TIM3 BV605, -TIGIT APC). A minimum of 500,000 PBMC was stained according to standard procedure. Cells were acquired by an acoustic focusing flow cytometer (Attune NxT, Thermo Fisher Scientific, Eugene, OR, USA), equipped with four lasers for excitation at 405, 488, 561 and 638 nm. Data were acquired in list mode using Attune NxT 2.4 software, and analyzed by FlowJo 9.9.6 (Ashland, OR, USA) under Mac OS X. Samples were compensated by software, after acquisition. Single staining and Fluorescence Minus One (FMO) controls were performed for all mAbs of the panel to set proper compensation and define positive signals. All cytofluorimetric analyses and cell sorting (see below) were performed according to the "Guidelines for the use of flow cytometry and cell sorting in immunological studies" [45].

Proliferation assay

Cells were stimulated for 6 days in resting conditions, i.e., treated with 10 ng/mL interleukin (IL)-7, or after stimulation with anti-CD3 plus anti-CD28 mAbs (1 µg/mL, Miltenyi Biotech, Bergisch Gladbach, Germany). The fluorescent dye 5,6-carboxyfluorescein diacetate succinimidyl ester (CFSE) was used at a concentration of 1 µg/mL (Life Technologies) according to standard procedures. Flow cytometric analyses for the identification of cycling cells belonging to different T cell populations were performed by gating T_N , T_{CM} , T_{EM} , T_{EMRA} among CD4+ and CD8+ T cells.

Intracellular cytokine detection

For functional assays, freshly isolated PBMCs were stimulated for 4 h at 37°C in a 5% CO₂ atmosphere with anti-CD3/CD28 (1 µg/mL), in complete culture medium (RPMI 1640 supplemented with 10% fetal bovine serum and 1% each of l-glutamine, sodium pyruvate, non-essential amino acids, antibiotics, 0.1 M HEPES, 55 µM β-mercaptoethanol) for 16 hours. For each sample, at least 2 million cells were left unstimulated as negative control and 2 million cells were stimulated. All samples were incubated with a protein transport inhibitor containing brefeldin A (Golgi Plug, BD). After stimulation, cells were stained with LIVE-DEAD Aqua (ThermoFisher Scientific) and surface mAbs recognizing CD3 PE-Cy5, CD4 AF700, and CD8 APC-Cy7 (Biolegend, San Diego, CA, USA). Cells were washed with stain buffer (BD) and fixed and permeabilized with the cytofix/cytoperm buffer set (BD) for cytokine detection. Then, cells were stained with mAbs recognizing IL-17 BV421, TNF-α BV603, IFN-γ FITC, or IL-4 APC (all mAbs from Biolegend), using previously described strategies for intracellular cytokine detection [5].

Mitochondrial bioenergetics and metabolic assays

CD4+ T_{EM} and T_N cells were sorted, seeded in triplicate at concentration of minimum 3.5×10^5 cells/well, rested for 4 h and stimulated for 16 h with anti-CD3 plus anti-CD28 as described above. Real time measurement of oxygen consumption rate (OCR) and extracellular acidification rate (ECAR) was performed by XF-96 Seahorse Extracellular Flux Analyzer (Agilent, Santa Clara, CA, USA) by using MitoStress Kit (Agilent) according to manufacturer's procedures. OCR was measured in XF media (non-buffered DMEM medium, containing 10 mM glucose, 2 mM L-glutamine, and 1 mM sodium pyruvate), under basal conditions and in response to 2 µM oligomycin, 1.5 µM of carbonylcyanide-4-(trifluoromethoxy)-phenylhydrazone (FCCP) and 1 µM of Antimycin and Rotenone (all from Sigma Aldrich). Indices of mitochondrial respiratory function were calculated from OCR profile: basal OCR (before addition of oligomycin), ATP-linked OCR (calculated as the difference between basal OCR rate and oligomycin-induced OCR rate) and maximal OCR (calculated as the difference of FCCP rate and antimycin plus rotenone rate) [46]. Moreover,

basal and maximal ECAR were measured. OCR and ECAR values were normalized to the number of cells per well.

Mitochondrial functionality, GLUT1 expression and mTOR activation from patients with different forms of MS

CD4⁺ T cells were sorted starting from 4×10^7 freshly isolated PBMC. Pure CD4⁺ cells were stimulated 16 h with anti-CD3 plus anti-CD28 or kept in resting condition with IL-7. After incubation, cells were stained with 200 nM Mitotracker Green or 50 nM Tetramethylrhodamine, Methyl Ester, Perchlorate (TMRM) (Thermo Fisher) according to standard procedures. After incubation, cells were washed and stained with mAbs CCR7-APC and CD45RA-PB (all from BioLegend). Cells were fixed and permeabilized according to standard procedure. Finally, cells were stained with mAb PE-conjugated for analyzing GLUT1 (Abcam, Cambridge, UK) expression or PE-conjugated S6 Ribosomal Protein (Ser235/Ser236) (eBioscience, San Diego, CA, USA) to evaluate the activation of mTOR. Regarding TMRM, results are expressed as TMRM Median Fluorescence Intensity (MFI) NS/ TMRM MFI S.

Analysis of the expression of genes related to glycolysis/mitochondrial respiration in T cells

A minimum of 1×10^7 PBMC was stained with anti-CD4 or anti-CD8 FITC (both from R&D), -CD45RA-PECy7 and -CCR7 PE (both from BioLegend). CD4⁺ and CD8⁺ T_{EM}, T_{CM} and T_N cells were sorted by using Biorad S3e Sorter (Bio-Rad, Hercules, CA, USA) with a purity >98%. Cells were rested for 4 h and then in vitro stimulated with anti-CD3 plus anti-CD28 (1 µg/mL) or kept with IL-7 (10 ng/mL, Miltenyi Biotech). After 4 h, RNA was extracted by using Quick-RNA Mini Prep (Zymo Research Corporation, Irvine, CA, USA), according to standard procedures. RNA concentration was determined by measuring absorbance at 260 nm using the NanoDrop ND-1000 (Thermo Scientific, Mississauga, ON, Canada). RNA was reverse-transcribed by cDNA synthesis kit (Bio-Rad), according to standard procedures. cDNA was pre-amplified with the SsoAdvanced PreAmp Supermix (Bio-Rad) and a pre-validated set of 8 pre-amplification assays (PrimePCR PreAmp assays, Bio-Rad). Seven key transcription factors involved in orchestrating the cellular metabolism were selected and quantified: c-Myc, HIF-1α, ERRα, BCL-6, FOXO1, KLF2 and MST1, along with TATA Binding Protein (TBP), used as reference gene; genes were quantified by using CFX96 Touch Real-Time PCR Detection System (Bio-Rad).

Western blotting analysis of proteins and phospho-proteins

Total cell lysates were obtained by standard methods. Protein concentrations were determined by Bradford Protein Assay (Bio-

Rad Laboratories). Then, 20 µg of total proteins were denatured for 5 minutes at 99°C using 4X Bolt LDS Sample Buffer (Life Technologies), separated using 12% precast gels (Life Technologies) and transferred onto a PVDF membrane (Bio-Rad). The Abs used were the following: anti-phospho-mTOR Ser2448, anti-mTOR, anti-phospho-AKT Ser473, anti-AKT (all 1:1000 dilution and from Cell Signaling Technology, Danvers, MA, USA), anti-TOM20 (1:1,000 from Santa Cruz Biotechnology, Dallas, Texas, USA), the filters were also probed with an actin antibody (1:1000 from Abcam, Cambridge, UK) to normalize for the amount of loaded protein. All primary antibody incubations were followed by incubation with Goat Anti-Rabbit IgG (HL)-HRP conjugated antibody (1:5,000, from Bio-Rad) and visualized using SuperSignal West Femto Maximum Sensitivity Substrate (Thermo Scientific, Rockford IL, USA) or Clarity Western ECL Substrate (Bio-Rad Laboratories) on a ChemiDoc MP (Bio-Rad). All filters were quantified using ImageLab 5.2.1, as previously described [47].

Transmission electron microscopy

Freshly isolated PBMC were sorted to obtain CD4⁺ T_{EM} and T_N cells. Cells were rested and stimulated as previously described. After 16 h of in vitro stimulation, pure T_{EM} and T_N cells were washed and cell pellets were obtained by centrifugation at 1200 rpm for 5 min. Cells were fixed in 2.5% glutaraldehyde in 0.1 M phosphate buffer (pH: 7.4) for 1 hour and postfixed in 1% OsO₄ for 1 h. Ultrathin sections, obtained from Durcupan embedded samples, were stained with UranylLess-lead citrate and then observed by a Zeiss EM109 transmission electron microscope (TEM). Randomly taken sections were examined for morphological analyses performed by Fiji software. Every single mitochondrion of the investigated cells was marked to analyze morphological characteristics: area, perimeter, major and minor axes. The most relevant descriptors of mt morphology i.e. aspect ratio (major axis/minor axis) form factor ($\text{perimeter}^2/4\pi \times \text{area}$), area and perimeter [48–51], were calculated and reported.

Pyruvate and lactate plasma level measurements

Blood was isolated by centrifugation at 800 rpm for 20 min at room temperature. Plasma was taken and centrifuged at 3500 rpm, 15 min, 4°C to eliminate platelets. Plasma was stored at -80°C until used. To measure pyruvate and lactate plasma levels, two colorimetric/fluorimetric kits were used, and manufacturer's procedures were followed (Pyruvate assay Kit and L-Lactate assay kit from AbCam, Cambridge UK).

Statistical analysis

Quantitative variables were compared with *t*-test (in case of repeated measures Wilcoxon *t*-test has been used, while for comparison between two groups Mann–Whitney *t*-test was applied). In the case of multiple comparisons, the Bonferroni correction was

applied. Simplified Presentation of Incredibly Complex Evaluation (SPICE) software (version 5.3, kindly provided by Dr. Mario Roederer, Vaccine Research Center, NIAID, NIH, Bethesda, MD, USA) was used to analyze polychromatic flow cytometry data, as described [5, 52]. Associations between clinical parameters and molecular data were sought using the Spearman Correlation test and logistic regression, as appropriate. Data are represented as the mean \pm SEM. Statistical analyses were performed using Prism 6.0 (GraphPad Software Inc., La Jolla, USA).

Acknowledgements: This work was funded by Italian Multiple Sclerosis Foundation (FISM) projects 2014/R/16 and 2016/R/20 to MP, and Fondazione Cassa di Risparmio di Vignola to MP. Sara De Biasi is a Marylou Ingram Scholar for the International Society for Advancement of Cytometry (ISAC). We thank Dr. Rosalberta Pullano (University of Modena and Reggio Emilia) for recruiting healthy subjects, Dr. Claudio Procaccini for Seahorse protocols, Dr. Luca Battistini for data discussion and Dr. Paola Paglia (ThermoFisher) for her technical support, and all the patients who donated their blood for these studies.

Conflict of interests: The authors declare no financial or commercial conflict of interest.

Author contributions: SDB performed most of the experiments; AMS, DF and PS selected and recruited patients and correlated clinical data with immunometabolic parameters; EB and DLT contributed to flow cytometry and WB analysis; SPe and MN performed gene expression analysis; SPa and PP analyzed OCR and ECAR; SDB, AMS, DF, AC and MP wrote the manuscript; MP coordinated the study.

References

- Leray, E., Yaouanq, J., Le Page, E., Coustans, M., Laplaud, D., Oger, J. and Edan, G., Evidence for a two-stage disability progression in multiple sclerosis. *Brain* 2010. **133**: 1900–1913.
- Mallucci, G., Peruzzotti-Jametti, L., Bernstock, J. D. and Pluchino, S., The role of immune cells, glia and neurons in white and gray matter pathology in multiple sclerosis. *Prog Neurobiol* 2015. **127–128**: 1–22.
- Frisullo, G., Plantone, D., Marti, A., Iorio, R., Damato, V., Nociti, V., Patanella, A. K. et al., Type 1 immune response in progressive multiple sclerosis. *J Neuroimmunol* 2012. **249**: 112–116.
- Zastepa, E., Fitz-Gerald, L., Hallett, M., Antel, J., Bar-Or, A., Baranzini, S., Lapierre, Y. et al., Naive CD4 T-cell activation identifies MS patients having rapid transition to progressive MS. *Neurology* 2014. **82**: 681–690.
- De Biasi, S., Simone, A. M., Nasi, M., Bianchini, E., Ferraro, D., Vitetta, F., Gibellini, L. et al., iNKT cells in secondary progressive multiple sclerosis patients display pro-inflammatory profiles. *Front Immunol* 2016. **7**: 555.
- Killestein, J., Den Drijver, B. F., Van der Graaff, W. L., Uitdehaag, B. M., Polman, C. H. and Van Lier, R. A., Intracellular cytokine profile in T-cell subsets of multiple sclerosis patients: different features in primary progressive disease. *Mult Scler* 2001. **7**: 145–150.
- Bianchini, E., De Biasi, S., Simone, A. M., Ferraro, D., Sola, P., Cossarizza, A. and Pinti, M., Invariant natural killer T cells and mucosal-associated invariant T cells in multiple sclerosis. *Immunol Lett* 2017. **183**: 1–7.
- MacIver, N. J., Michalek, R. D. and Rathmell, J. C., Metabolic regulation of T lymphocytes. *Annu Rev Immunol* 2013. **31**: 259–283.
- Pearce, E. L., Metabolism in T cell activation and differentiation. *Curr Opin Immunol* 2010. **22**: 314–320.
- Wahl, D. R., Byersdorfer, C. A., Ferrara, J. L., Otipari, A. W., Jr. and Glick, G. D., Distinct metabolic programs in activated T cells: opportunities for selective immunomodulation. *Immunol Rev* 2012. **249**: 104–115.
- Gerriets, V. A. and Rathmell, J. C., Metabolic pathways in T cell fate and function. *Trends Immunol* 2012. **33**: 168–173.
- O'Neill, L. A., Kishton, R. J. and Rathmell, J., A guide to immunometabolism for immunologists. *Nat Rev Immunol* 2016. **16**: 553–565.
- Carbone, F., De Rosa, V., Carrieri, P. B., Montella, S., Bruzzese, D., Porcellini, A., Procaccini, C. et al., Regulatory T cell proliferative potential is impaired in human autoimmune disease. *Nat Med* 2014. **20**: 69–74.
- Venken, K., Hellings, N., Hensen, K., Rummens, J. L., Medaer, R., D'Hooghe M., Dubois, B. et al., Secondary progressive in contrast to relapsing-remitting multiple sclerosis patients show a normal CD4+CD25+ regulatory T-cell function and FOXP3 expression. *J Neurosci Res* 2006. **83**: 1432–1446.
- van der Windt, G. J. and Pearce, E. L., Metabolic switching and fuel choice during T-cell differentiation and memory development. *Immunol Rev* 2012. **249**: 27–42.
- Rathmell, J. C., Vander Heiden, M. G., Harris, M. H., Frauwirth, K. A. and Thompson, C. B., In the absence of extrinsic signals, nutrient utilization by lymphocytes is insufficient to maintain either cell size or viability. *Mol Cell* 2000. **6**: 683–692.
- Rathmell, J. C., Farkash, E. A., Gao, W. and Thompson, C. B., IL-7 enhances the survival and maintains the size of naive T cells. *J Immunol* 2001. **167**: 6869–6876.
- Jacobs, S. R., Michalek, R. D. and Rathmell, J. C., IL-7 is essential for homeostatic control of T cell metabolism in vivo. *J Immunol* 2010. **184**: 3461–3469.
- Sena, L. A., Li, S., Jairaman, A., Prakriya, M., Ezponda, T., Hildeman, D. A., Wang, C. R. et al., Mitochondria are required for antigen-specific T cell activation through reactive oxygen species signaling. *Immunity* 2013. **38**: 225–236.
- Dendrou, C. A., Fugger, L. and Friese, M. A., Immunopathology of multiple sclerosis. *Nat Rev Immunol* 2015. **15**: 545–558.
- Sospedra, M. and Martin, R., Immunology of multiple sclerosis. *Annu Rev Immunol* 2005. **23**: 683–747.
- Buck, M. D., O'Sullivan, D. and Pearce, E. L., T cell metabolism drives immunity. *J Exp Med* 2015. **212**: 1345–1360.
- De Riccardis, L., Rizzello, A., Ferramosca, A., Urso, E., De Robertis, F., Danielli, A., Giudetti, A. M. et al., Bioenergetics profile of CD4(+) T cells in relapsing remitting multiple sclerosis subjects. *J Biotechnol* 2015. **202**: 31–39.
- Ontaneda, D., Thompson, A. J., Fox, R. J. and Cohen, J. A., Progressive multiple sclerosis: prospects for disease therapy, repair, and restoration of function. *Lancet* 2017. **389**: 1357–1366.
- Sallusto, F., Lenig, D., Forster, R., Lipp, M. and Lanzavecchia, A., Two subsets of memory T lymphocytes with distinct homing potentials and effector functions. *Nature* 1999. **401**: 708–712.

- 26 Pinti, M., Cevenini, E., Nasi, M., De Biasi, S., Salvioli, S., Monti, D., Benatti, S. et al., Circulating mitochondrial DNA increases with age and is a familiar trait: Implications for “inflamm-aging”. *Eur J Immunol* 2014. **44**: 1552–1562.
- 27 Pender, M. P., Csurhes, P. A., Pfluger, C. M. and Burrows, S. R., Deficiency of CD8⁺ effector memory T cells is an early and persistent feature of multiple sclerosis. *Mult Scler* 2014. **20**: 1825–1832.
- 28 Pearce, E. L., Walsh, M. C., Cejas, P. J., Harms, G. M., Shen, H., Wang, L. S., Jones, R. G. et al., Enhancing CD8 T-cell memory by modulating fatty acid metabolism. *Nature* 2009. **460**: 103–107.
- 29 Pearce, E. L., Poffenberger, M. C., Chang, C. H. and Jones, R. G., Fueling immunity: insights into metabolism and lymphocyte function. *Science* 2013. **342**: 1242454.
- 30 Weinberg, S. E., Sena, L. A. and Chandel, N. S., Mitochondria in the regulation of innate and adaptive immunity. *Immunity* 2015. **42**: 406–417.
- 31 O’Sullivan, D., van der Windt, G. J., Huang, S. C., Curtis, J. D., Chang, C. H., Buck, M. D., Qiu, J. et al., Memory CD8(+) T cells use cell-intrinsic lipolysis to support the metabolic programming necessary for development. *Immunity* 2014. **41**: 75–88.
- 32 Corrado, M. and Campello, S., Autophagy inhibition and mitochondrial remodeling join forces to amplify apoptosis in activation-induced cell death. *Autophagy* 2016. **12**: 2496–2497.
- 33 Tal, M. C., Sasai, M., Lee, H. K., Yordy, B., Shadel, G. S. and Iwasaki, A., Absence of autophagy results in reactive oxygen species-dependent amplification of RLR signaling. *Proc Natl Acad Sci U S A* 2009. **106**: 2770–2775.
- 34 Buck, M. D., O’Sullivan, D., Klein Geltink, R. I., Curtis, J. D., Chang, C. H., Sanin, D. E., Qiu, J. et al., Mitochondrial dynamics controls T cell fate through metabolic programming. *Cell* 2016. **166**: 63–76.
- 35 Menk, A. V., Scharping, N. E., Moreci, R. S., Zeng, X., Guy, C., Salvatore, S., Bae, H. et al., Early TCR signaling induces rapid aerobic glycolysis enabling distinct acute T cell effector functions. *Cell Rep* 2018. **22**: 1509–1521.
- 36 Doedens, A. L., Phan, A. T., Stradner, M. H., Fujimoto, J. K., Nguyen, J. V., Yang, E., Johnson, R. S. et al., Hypoxia-inducible factors enhance the effector responses of CD8(+) T cells to persistent antigen. *Nat Immunol* 2013. **14**: 1173–1182.
- 37 Shi, L. Z., Wang, R., Huang, G., Vogel, P., Neale, G., Green, D. R. and Chi, H., HIF1alpha-dependent glycolytic pathway orchestrates a metabolic checkpoint for the differentiation of TH17 and Treg cells. *J Exp Med* 2011. **208**: 1367–1376.
- 38 Michalek, R. D., Gerriets, V. A., Jacobs, S. R., Macintyre, A. N., MacIver, N. J., Mason, E. F., Sullivan, S. A. et al., Cutting edge: distinct glycolytic and lipid oxidative metabolic programs are essential for effector and regulatory CD4⁺ T cell subsets. *J Immunol* 2011. **186**: 3299–3303.
- 39 Laplante, M. and Sabatini, D. M., mTOR signaling in growth control and disease. *Cell* 2012. **149**: 274–293.
- 40 Pucino, V., Bombardieri, M., Pitzalis, C. and Mauro, C., Lactate at the crossroads of metabolism, inflammation, and autoimmunity. *Eur J Immunol* 2017. **47**: 14–21.
- 41 Albanese, M., Zagaglia, S., Landi, D., Boffa, L., Nicoletti, C. G., Marciani, M. G., Mandolesi, G. et al., Cerebrospinal fluid lactate is associated with multiple sclerosis disease progression. *J Neuroinflammation* 2016. **13**: 36.
- 42 Haas, R., Smith, J., Rocher-Ros, V., Nadkarni, S., Montero-Melendez, T., D’Acquisto, F., Bland, E. J. et al., Lactate regulates metabolic and pro-inflammatory circuits in control of T cell migration and effector functions. *PLoS Biol* 2015. **13**: e1002202.
- 43 Fischer, K., Hoffmann, P., Voelkl, S., Meidenbauer, N., Ammer, J., Edinger, M., Gottfried, E. et al., Inhibitory effect of tumor cell-derived lactic acid on human T cells. *Blood* 2007. **109**: 3812–3819.
- 44 Lublin, F. D., Reingold, S. C., Cohen, J. A., Cutter, G. R., Sorensen, P. S., Thompson, A. J., Wolinsky, J. S. et al., Defining the clinical course of multiple sclerosis: the 2013 revisions. *Neurology* 2014. **83**: 278–286.
- 45 Cossarizza, A., Chang, H. D., Radbruch, A., Akdis, M., Andra, I., Annunziato, F., Bacher, P. et al., Guidelines for the use of flow cytometry and cell sorting in immunological studies. *Eur J Immunol* 2017. **47**: 1584–1797.
- 46 Procaccini, C., Carbone, F., Di Silvestre, D., Brambilla, F., De Rosa, V., Galgani, M., Faicchia, D. et al., The proteomic landscape of human ex vivo regulatory and conventional T cells reveals specific metabolic requirements. *Immunity* 2016. **44**: 406–421.
- 47 Gibellini, L., Pinti, M., Bartolomeo, R., De Biasi, S., Cormio, A., Musicco, C., Carnevale, G. et al., Inhibition of Lon protease by triterpenoids alters mitochondria and is associated to cell death in human cancer cells. *Oncotarget* 2015. **6**: 25466–25483.
- 48 Krebichl, G., Ruckerbauer, S., Burbulla, L. F., Kieper, N., Maurer, B., Waak, J., Wolburg, H. et al., Reduced basal autophagy and impaired mitochondrial dynamics due to loss of Parkinson’s disease-associated protein DJ-1. *PLoS One* 2010. **5**: e9367.
- 49 Koopman, W. J., Visch, H. J., Smeitink, J. A. and Willems, P. H., Simultaneous quantitative measurement and automated analysis of mitochondrial morphology, mass, potential, and motility in living human skin fibroblasts. *Cytometry A* 2006. **69**: 1–12.
- 50 Santulli, G., Xie, W., Reiken, S. R. and Marks, A. R., Mitochondrial calcium overload is a key determinant in heart failure. *Proc Natl Acad Sci U S A* 2015. **112**: 11389–11394.
- 51 Picard, M., White, K. and Turnbull, D. M., Mitochondrial morphology, topology, and membrane interactions in skeletal muscle: a quantitative three-dimensional electron microscopy study. *J Appl Physiol* 1985 2013. **114**: 161–171.
- 52 De Biasi, S., Bianchini, E., Nasi, M., Digaetano, M., Gibellini, L., Carnevale, G., Borghi, V. et al., Th1 and Th17 proinflammatory profile characterizes invariant natural killer T cells in virologically suppressed HIV+ patients with low CD4⁺/CD8⁺ ratio. *AIDS* 2016. **30**: 2599–2610.

Abbreviations: CM: central memory · CTR: controls · EM: effector memory · EMRA: effector memory re-expressing CD45RA · N: naïve · PP: primary progressive · SP: secondary progressive

Full correspondence: Prof. Marcello Pinti, Department of Life Sciences, University of Modena and Reggio Emilia, Via G. Campi 287, 41125, Modena (MO), Italy
Fax: +39 059 205 5426
e-mail: marcello.pinti@unimore.it

Additional correspondence: Dr. Sara De Biasi, Department of Life Sciences, University of Modena and Reggio Emilia, Via G. Campi 287, 41125, Modena (MO), Italy
Fax: +39 059 205 5426
e-mail: debiasisara@yahoo.it

The peer review history for this article is available at <https://publons.com/publon/10.1002/eji.201948223>

Received: 24/4/2019

Revised: 28/6/2019

Accepted article online: 2/8/2019